Mesozoic Tectonics of the Maria Belt, west-central Arizona and southeastern California

STEPHEN M. RICHARD, Arizona Geological Survey, 845 N. Park Ave., Tucson AZ 85719
STANTON N. BALLARD, 3213 Rankin, Dallas TX 75205
STEFAN S. BOETTCHER, Dept. of Geological Sciences, University of Texas, Austin TX 78712
WARREN B. HAMILTON, U.S. Geological Survey, MS 964, Box 25046 Federal Center, Denver CO 80225
THOMAS D. HOISCH, Dept. of Geology, Northern Arizona University, Box 4099, Flagstaff AZ 86011
RICHARD M. TOSDAL, U.S. Geological Survey,MS 901, 345 Middlefield Rd, Menlo Park CA 94025

INTRODUCTION

Location

The Maria belt in west-central Arizona and southeastern California is part of an east-trending deformation zone situated between the thrust belts of southern Nevada and Chihuahua (Figure 1). Rocks in this region record a complex Mesozoic history including local Triassic(?) erosioh of the entire Paleozoic section, Jurassic magmatism, and Jurassic to Cretaceous high-angle faulting, basin formation, thrust faulting and normal faulting. Complex superposed deformation is the rule, typically including early southward tilting or formation of southward-facing folds and later top-to-the-northeast or top-to-the-southwest movement on low-angle faults. The exact sequence of events varies from range to range, and the large-scale kinematics are debatable.

The Maria belt has three major components: (1)a thick south-dipping section of Jurassic volcanic and volcaniclastic rocks overlain by up to 8 km of Jurassic(?) or Cretaceous McCoy Mountains Formation [Miller, 1944; Harding and Coney, 1985; Stone and others, 1987] is bounded by (2) the Maria fold and thrust belt [Reynolds and others, 1986; Spencer and Reynolds, 1990] on the north, and by (3) the Mule Mountains thrust system on the south [Tosdal, 1991]. Rocks north of and within the Maria fold and thrust belt include the following: (1) a basement of Precambrian metamorphic and granitic rocks; (2) cratonic Paleozoic and lower Mesozoic strata 1-1.5 km thick, correlated with units of similar age on the Colorado Plateau; (3) Jurassic granitoids; (4) up to 2 km of intermediate to felsic volcanic rocks of probable Jurassic age; (5) up to 8 km of Jurassic(?) or Cretaceous clastic rocks, broadly correlative with the McCoy Mountains Formation and (6) mostly

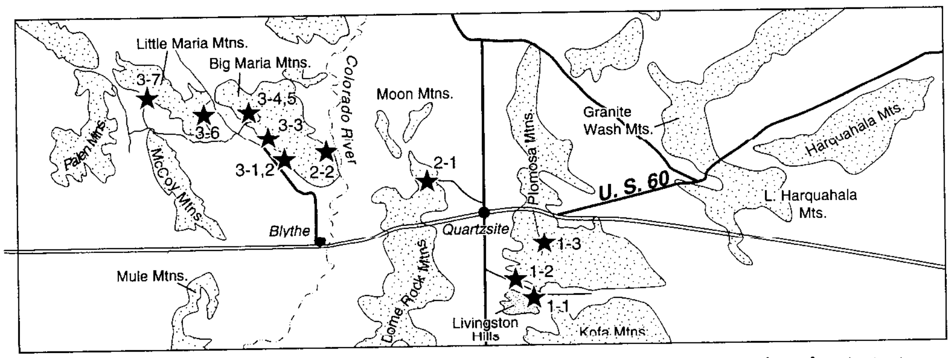

Figure 1. Map of the Maria belt showing location of stops and mountain ranges referred to in text.

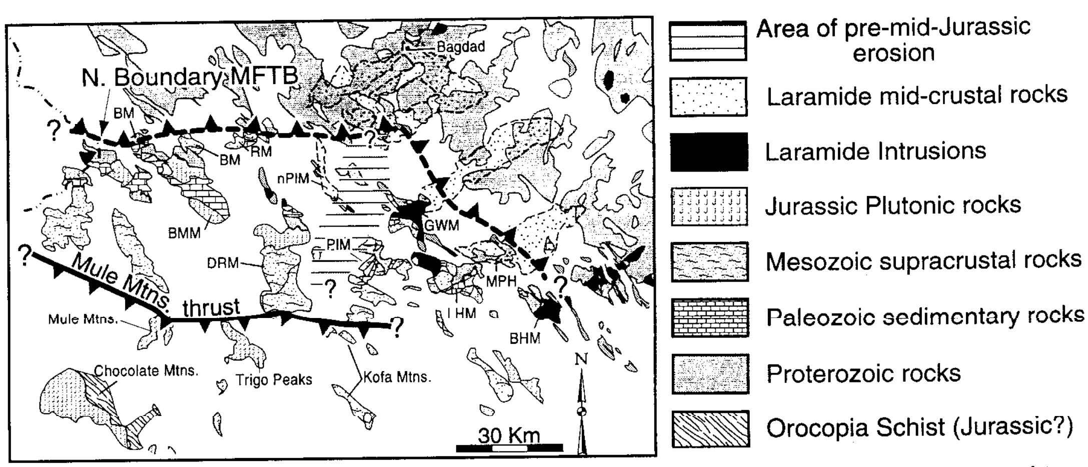

Figure 2. Palinspastic reconstruction of the Maria belt region for the early Tertiary. Post-late Cretaceous (Laramide) rocks are not shown. Arizona geology from Reynolds, 1988; geology in California from Jennings, 1977 and this report. Laramide mid-crustal rocks are presently exposed in the footwall of major middle Tertiary detachment faults. The trace of the northern limit of the Maria Fold and thrust belt (MFTB) is the approximate northern limit of greenschist-facies Paleozoic and Mesozoic supracrustal rocks preserved beneath Proterozoic crystalline rocks in the hanging wall of thrust faults. The present trace of the Colorado River relative to the Colorado Plateau is shown for reference. Abbreviations: BHM-Big Horn Mountains, BM-Buckskin Mountains (rocks above detachment fault), BMM-Big Maria Mountains, DRM-Dome Rock Mountains, GWM-Granite Wash Mountains, LHM-Little Harquahala Mountains, MFTB-Maria fold and thrust belt, MPH-Merrit Pass Hills, nPIM-northern Plomosa Mountains, PIM-Plomosa Mountains, RM-Rawhide Mountains.

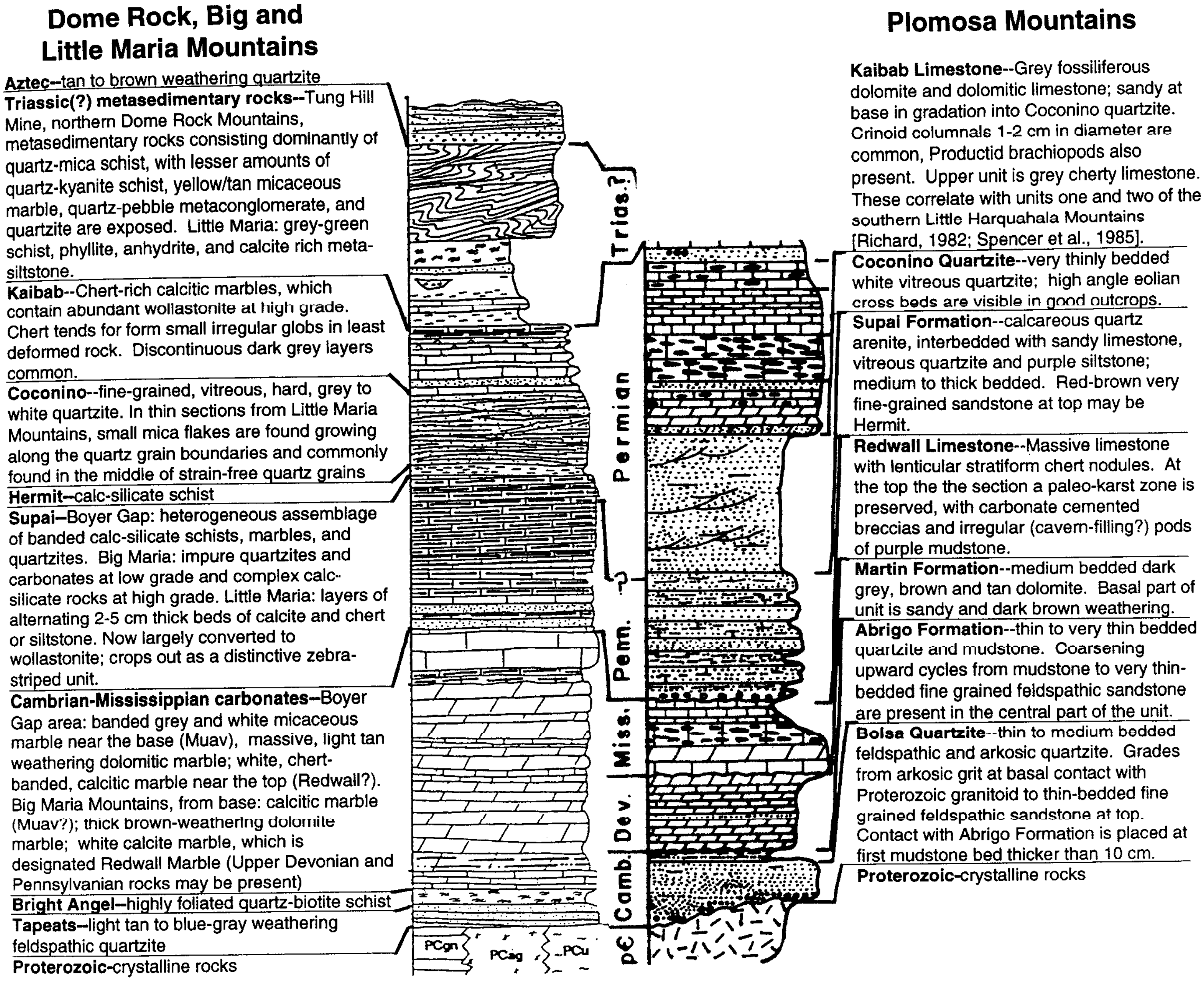

Figure 3. Paleozoic and lower Mesozoic stratigraphy of eastern (Plomosa Mountains) and western (Big and Little Maria mountains) Maria fold and thrust belt.

undeformed Late Cretaceous plutons. These rocks will be the focus of our field trip.

Early Miocene and probable Late Cretaceous or early Tertiary low-angle normal faults have unroofed deeper structural levels from south to north or southwest to northeast. The deepest structural levels are exposed beneath the Miocene Whipple-Buckskin-Bullard detachment fault system at the eastern end of the belt. Significant Miocene normal faults in the northern part of the Big Maria, Dome Rock and Plomosa mountains apparently lose displacement southward [Spencer and Reynolds, 1989, 1991]. Large-scale tilting of uncertain magnitude accompanied movement on these faults, but the ranges we will visit are largely unextended internally and appear to form a 'raft' separating regions of greater mid-Tertiary extension to the north, east and south [Sherrod and Tosdal, 1991; Spencer and Reynolds, 1991]. The western end of the Maria belt has been disrupted by Late Miocene right-slip faulting [Richard, 1993]. In order to facilitate discussion of Mesozoic tectonics, Figure 2 presents a palinspastic reconstruction of the Maria Belt in early Tertiary time.

Purpose of trip

On this trip, we will examine faults and unconformities in the Cretaceous McCoy Mountains Formation and related rocks representing shallow paleodepth in the southern Plomosa Mountains and Livingston Hills, and poly-deformed Paleozoic and Mesozoic metasedimentary rocks representing deeper parts of the orogen in the northern Dome Rock, Big Maria and Little Maria Mountains. Major problems to be addressed include the interaction of deformation and sedimentation at high structural levels in the southern part of the belt, style and kinematics of ductile deformation in the northern part of the belt, and the relationship between events documented in these two domains.

OVERVIEW OF ROCK UNITS

Stone and Pelka (1989)	Harding and Coney (1985)	Tosdal and Stone, 1994	this report	lithology
Member L	Not exposed ???	Not exposed		
Member K	Siltstone member		? ? ? ? ?	
Member J				
Member I				
Member H				
Member G ●		???	Upper unit	fining upward sequence from conglomerate to sandstone to siltstone; sandstone lithofeldspathic; conglomerate polymict, source to north.
Member F	● Sandstone member	Upper unit		
	⊘ Conglomerate member			
Member E	Mudstone member	Lower unit	unit 2	heterogeneous conglomerate sandstone and siltstone or mudstone; volcanic-lithic sandstone common in lower part; in some sections, mudstone in upper part grades up into conglomerate
Member D	Basal sandstone member 2			
Member C				
Member B	Basal sandstone member 1		unit 1	quartz arenite, quartzite-cobble conglomerate and maroon siltstone
Member A				

⊘ U-Pb sample location ● Fossil angiosperm

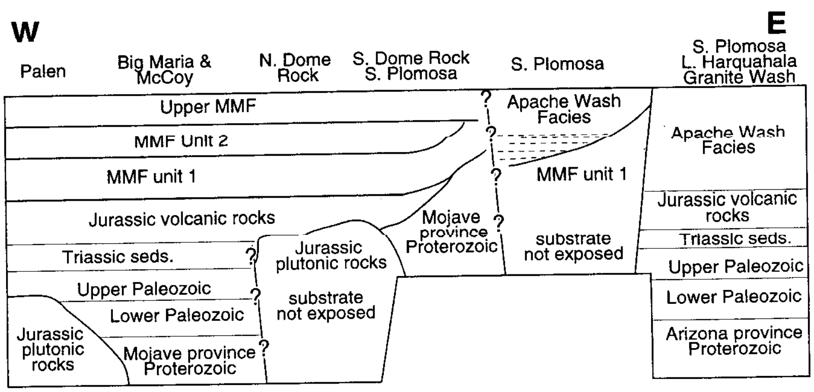

Figure 4. A. Correlation of proposed stratigraphic nomenclature for the McCoy Mountains Formation. B. Schematic lithostratigraphic cross section along the Maria Belt.

Proterozoic rocks consist of Early Proterozoic metavolcanic and metasedimentary rocks and granitoids intruded by coarse-grained Middle Proterozoic granitoids. These are overlain by 1 to 2 km of Paleozoic and lower Mesozoic quartz-rich sandstone, carbonates and shale (Figure 3). Cambrian-Devonian carbonate units appear to change character significantly between the eastern Plomosa Mountains and the northern Dome Rock Mountains.

One or more episodes of deformation affected Paleozoic and Proterozoic rocks before the onset of thrust faulting in the Cretaceous [Reynolds and others, 1989]. These events are now recorded only by unconformities and coarse conglomerates. These pre-existing structures may have significantly affected the location and stratigraphic separation of younger thrust faults, but pre-thrusting faults, if present, are difficult to recognize due to the complex deformation history. A narrow north-trending domain in which lower Mesozoic strata directly overlie Proterozoic rocks is centered on Quartzsite, and can be traced as far north as the southwestern Buckskin Mountains (Figure 2). This domain appears to separate the two types of Paleozoic section indicated in Figure 3.

Thick sequences of Middle Jurassic dacitic to rhyolitic pyroclastic rocks, minor lavas, and volcaniclastic rocks in the Maria belt are collectively referred to as the Middle Jurassic Dome Rock sequence [Tosdal and others, 1989]. The thickest preserved section, in the central Dome Rock Mountains is a minimum of about 4 km thick. U-Pb ages are typically between 175 and 158 Ma from stratigraphically equivalent rocks in several parts of the Maria belt, as well as elsewhere in southern Arizona and southern California [Reynolds and others, 1987; Graubard and others, 1988; Busby-Spera and others, 1990; Riggs and others, 1993; R.M. Tosdal, unpublished data, 1993].

The intrusive component of the Jurassic magmatic arc is represented by a compositionally-expanded suite of granitoids collectively known as the Kitt Peak-Trigo Peak superunit [Tosdal and others, 1989]. The granitoids are metaluminous and calc-alkaline with a tendency toward an alkalic character (high K_2O). They are subdivided into three plutonic units, which have similar petrologic, chemical, and chronologic characteristics over some 500 km from the easternmost Transverse Ranges in southern California to the Baboquivari Mountains in southern Arizona. The oldest plutonic unit is heterogeneous, ranging from hornblendite to granite (~45%-74% SiO2), but diorite is most typical. Available U-Pb data indicate ages of about 173 to 170 Ma [R.M. Tosdal, unpublished data 1993], essentially the same age as the lower part of the Dome Rock sequence. Porphyritic granodiorite, with subordinate quartz monzodiorite and granite, form the second intrusive unit. In contrast to the diorite unit, the porphyritic granodiorite is relatively homogeneous (60%-69% SiO2) and is typified by conspicuous K-feldspar phenocrysts. These rocks give U-Pb ages of 165-163 Ma in 9 ranges in the region [Tosdal and others, 1989; R.M. Tosdal, unpublished data 1993]. The youngest plutonic unit consists of homogeneous leucogranite (70%-77% SiO2) that intrudes older rocks primarily as dikes, sills, or small plutons. The older units of the suite are typically weakly to strongly deformed, but late leucocratic granitoids are commonly undeformed. Uncertainties cloud the tectonics of deformation affecting these units, but one generation of folds in the Boyer Gap area is intruded by granite. U-Pb isotopic data indicate that the granites are 160 to 158 Ma, essentially the same age as the upper Dome Rock sequence.

The age, correlation, and tectonic setting of the McCoy Mountains Formation (MMF) [Miller, 1944] and related rocks has been the topic of much debate. This thick sequence (as much as 8 km) of continental clastic rocks buried the Jurassic magmatic arc in western Arizona and southeastern California, and in the Blythe-Quartzsite region contains the only record of some 90 m.y. between Jurassic volcanism and the reinception of deformation, regional metamorphism and plutonism in the Late Cretaceous. The McCoy Mountains Formation has been divided into two units, a quartzose- and volcaniclastic-rich lower unit and a feldspathic upper unit [Tosdal and others, 1989; Tosdal and Stone, 1994] (Figure 4). An unconformity separates these two units in the southern Plomosa and Dome Rock Mountains and the Livingston Hills. The lower unit records the degradation of the subjacent silicic volcanic arc and is

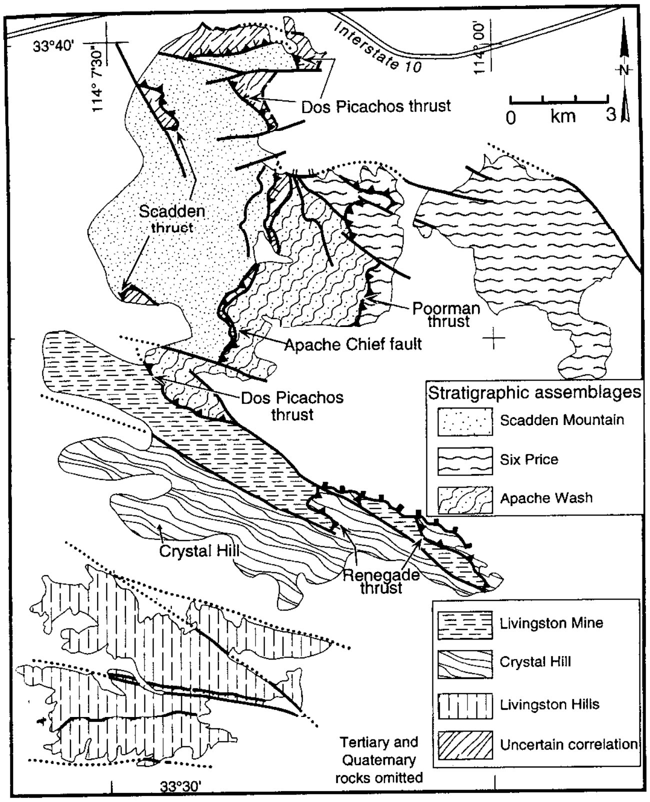

Figure 5. Structural-stratigraphic domains in the southern Plomosa Mountains. Geology from Richard and others [1993], Sherrod and others [1990] and Tosdal and Stone [1994].

considered to be of Jurassic(?) and Cretaceous age [Tosdal and Stone, 1994]. These strata are probably correlative with the Upper Jurassic and Lower Cretaceous Bisbee Group in southeastern Arizona [Dickinson and other, 1989]. In contrast, the upper unit is interpreted to be of Late Cretaceous age and has been proposed to represent a foreland basin deposit shed from the rising and evolving Maria fold and thrust belt [Stone and others, 1987; Tosdal and Stone, 1994].

The lower unit of the MMF of Tosdal and others [1989] is subdivided here into a quartz-arenite-rich unit 1 and a heterogeneous unit 2 (roughly corresponding to basal unit 1 and basal unit 2 plus mudstone members of Harding and Coney [1985]) (Figure 4). The lower quartzose unit and the upper unit are recognizable from range to range, but the intervening unit (basal unit 2 and mudstone member of Harding and Coney [1985] and unit 2 of this report) varies greatly in lithology and stratigraphy. Quartz arenite of the lower unit (basal sandstone member 1 of Harding and Coney [1985]) is one of the most distinctive rock units in the region, and is present from the southern Little Harquahala Mountains [Richard and others, 1987] to the Palen Mountains [Pelka, 1973], and southward some 70 km south along the Colorado River in the area west of Laguna Dam [Richard, 1992a]. The generally upward-fining sequence and feldspathic character of the upper unit (conglomerate, sandstone, siltstone members of Harding and Coney [1985]) is also distinctive. The stratigraphically heterogeneous rocks above quartzose-rich unit 1 and below massive conglomerate or sandstone at the base of the upper unit make regional subdivision of this interval difficult.

Clastic sequences that overlie Paleozoic strata in the eastern part of the belt may correlate with either heterogeneous unit 2 or with the upper unit of the MMF. Referred to as Apache Wash facies [Reynolds and others, 1986; Richard and others, 1987], these sequences are characterized by a large proportion of lithofeldspathic sandstone, and the local abundance of mafic sills. Two sections show a well developed fining-upward stratigraphy (Apache Wash, southern Little Harquahala Mtns.), but in other sections there is no clear pattern of fining or coarsening (Ramsay Mine, Granite Wash Mtns.). Fine-grained sandstone in the upper part of the Apache Wash section depositionally overlies unit 1 of the MMF, demonstrating that these rocks are not older than the MMF. The Granite Wash granodiorite, which has yielded an $^{40}Ar/^{39}Ar$ hornblende plateau age of 80 Ma [S.M. Richard, unpublished data, 1992], intrudes rocks of the Granite Wash section.

GEOLOGY OF MOUNTAIN RANGES IN THE BLYTHE-QUARTZSITE AREA

Livingston Hills (Tosdal)

Conglomerate, sandstone and siltstone of the upper McCoy Mountains Formation that underlie the Livingston Hills are folded into a north-facing, gently east-plunging syncline, which is broken by thrust faults parallel to its axial surface. North-verging folding of the sedimentary rocks is related to northward-directed transport in the footwall of the latest Cretaceous Mule Mountains thrust system [Tosdal, 1990].

In the northeastern Livingston Hills quartz arenite and maroon siltstone of MMF unit 1 are unconformably overlain on the south by steeply dipping, distinctive, granite-clast conglomerate [Tosdal and Stone, 1994] (Stop 1-1). At the NW tip of the Livingston Hills, upright and south-facing conglomerate and minor sandstone of the conglomerate member is in contact with an isolated and upright section of lithofeldspathic sandstone, pebble conglomerate, and minor siliceous siltstone and limestone assigned to heterogeneous unit 2 of the MMF [Tosdal and Stone, 1994]. Clasts of unit 2 are present in the conglomerate. Field relations suggest that the contact between the upper and lower units of the MMF at this locality is either an angular unconformity or a premetamorphic fault.

The structural orientation of the largely south-dipping upper MMF conglomerate is similar in both areas, but the 1,000-m-thick section of polymictic conglomerate that underlies the distinctive granite-clast conglomerate in the northwestern Livingston Hills is absent in the northeastern Livingston Hills (Stop 1-1). Tosdal and Stone [1994] interpreted these relations to indicate that MMF unit 1 was faulted against heterogeneous unit 2 before deposition of the upper MMF conglomerate, which then overlapped the fault contact between those units. The abrupt westward thickening of the upper MMF conglomerate indicates a down-to-the-southwest component of movement on this fault. This fault is interpreted as a thrust fault because the overturned bedding in the Crystal Hill area implies contraction, and because the fanning dips in the upper MMF conglomerate in the northwestern Livingston Hills suggests that these rocks could have been deposited synchronously with a reverse growth fault or above a blind thrust. The present fault, which cuts the conglomerate, would be the result of continued movement or reactivation.

Plomosa Mountains (Richard)

Six contrasting Mesozoic stratigraphic assemblages characterize fault-bounded terranes in the southern Plomosa

Mountains (Figure 5, 6). The kinematics of high- and low-angle faults bounding the stratigraphic domains are poorly constrained, hindering reconstruction of their pre-faulting configuration. Likewise, the sedimentological characteristics of the stratigraphic sequences do not dictate their original configuration. Many of the domain-bounding faults appear to have polyphase histories.

Pre-thrusting deformation is recorded by unconformities and coarse sedimentary deposits. In the Scadden Mountain block, lower Mesozoic conglomerate is deposited directly on Proterozoic metavolcanic rocks [Lerch, 1990]. These sediments are overlain conformably by Jurassic volcanic rocks. Conglomerate at the base of unit 1 of the MMF onlaps across these Jurassic volcanic rocks to directly overlie Proterozoic granitoid. Dramatic changes in the thickness of Jurassic ash-flow tuff units may be due to volcano-tectonic subsidence or eruption of tuffs onto pre-exisiting topography. Quartzite breccias (Pc?) in Jurassic tuff blocks in the Apache Wash breccia may record caldera collapse. Megabreccia in the Apache Wash sequence was deposited from a sourçe to the south, presently not exposed or removed by subsequent fault slip or erosion. This source may be related to the old northwest-trending faults, or record an even older deformation event.

The most prominent structures are a series of gently-dipping thrust faults. Fault names used here are those proposed in Reynolds and others [1986]. The Poorman thrust is a minor imbrication between the Six Price and Apache Wash blocks. A minimum of 4 km of SSW transport of the hanging wall is necessary to produce the observed separation of the cut off of steeply SE-dipping Paleozoic strata at the northwest-trending pre-Poorman high-angle fault (Figure 7). The Dos Picachos thrust is the major fault between the Apache Wash and Scadden Mountain blocks because of the greater development of tectonite fabric along this contact than along the Apache Chief thrust. Data available are insufficient to determine its direction of transport on the Dos Picachos thrust. The nature of the Apache Chief thrust, which places the Paleozoic and Jurassic-block chaos/megabreccia unit on top of unit 1 of the MMF, is cryptic. It may be a significant pre-Dos Picachos fault or a disrupted depositional contact. We suggest that this contact be referred to as the Apache Chief fault rather than thrust because of this uncertainty.

Two major lithologic discontinuities in the southern Plomosa Mountains are northwest-trending high(?)-angle faults that pre-date thrust faults in the area. A pre-Poorman-thrust, northwest-trending high-angle fault (now largely overprinted by minor Tertiary normal slip) is the major structure that juxtaposes the Six Price and Apache Wash blocks. This fault does not displace the Dos Picachos thrust along the east side of Scadden Mountain and is inferred to be older. The southern part of the Dos Picachos thrust overlaps an inferred fault contact between the Scadden Mountain and Livingston Mine blocks. This pre-Dos Picachos fault is constrained by outcrop distribution to have a northwest trend similar to that of the pre-Poorman high-angle fault. This older fault does not outcrop but is inferred from the stratigraphic contrast between the Scadden Mountain sequence and Livingston Mine sequence, and the change from a relatively high stratigraphic position in MMF unit 2 north of the discontinuity to the base of a very thick sequence of Jurassic volcanic rocks on the south side. Miller and McKee's [1971] interpretation that major northwest-trending strike slip faults are present remains valid, but the faults are pre-Tertiary.

Within the Crystal Hill block, a complex zone of folding and faulting separates the eastern part of the block, characterized by a simple, south- to SSW-dipping upright homocline from the western part, which is a NNW-dipping overturned homocline. This deformation zone starts about 1 km east of Crystal Hill. NW- to W-dipping cleavage in the deformation zone is apparently axial planar to a pinched syncline cored by conglomerate (W of center, sec 11, T2N R18W). Conglomerate overlies overturned Crystal Hill formation depositionally, and the cleavage formation thus post

Figure 6. Stratigraphy of domains in the southern Plomosa Mountains. Location of domains shown in Figure 5. Abbreviations: MMF-McCoy Mountains Formation.

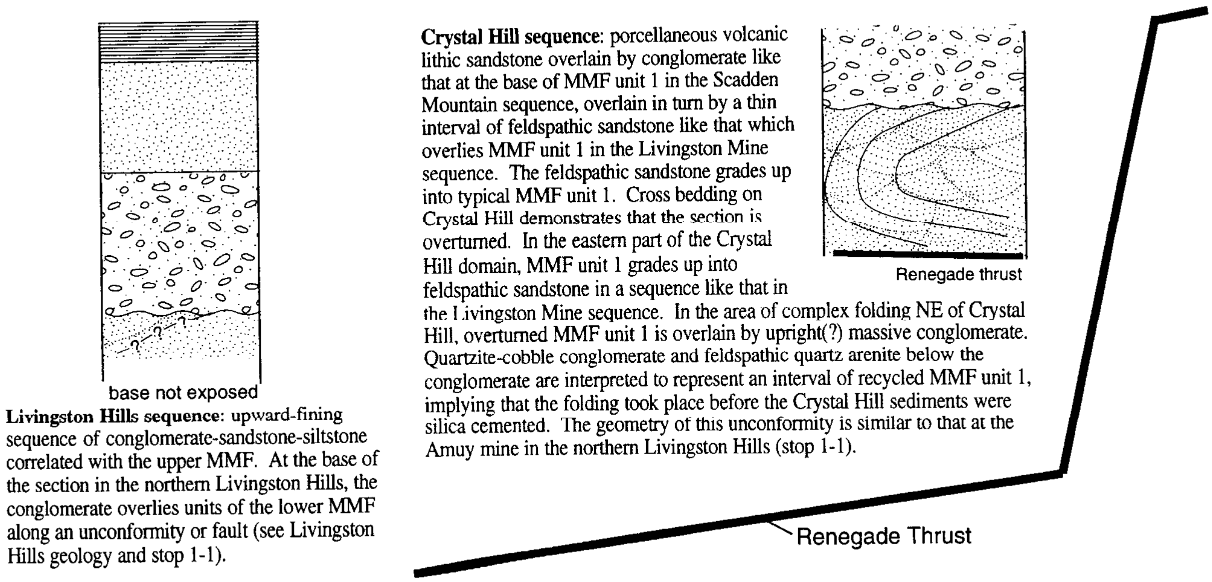

dates the overturning of section at Crystal Hill.

Early Miocene northeast- to east-trending faults along lower Apache Wash, and northwest-trending faults in the central and southern part of the map area disrupt the older structures, and are apparently mostly normal faults, but amounts of slip are poorly constrained. Miocene basalt overlaps these faults.

Dome Rock Mountains (Tosdal)

The Dome Rock Mountains contain a near-continuous cross-section through the varied elements of the Mesozoic arc in the Blythe-Quartzsite area (Figure 8). Two inward-facing Cretaceous synclinoria are located at the northern and southern ends of the range, with principally Jurassic and Cretaceous igneous and sedimentary rocks lying in the intervening area. Tertiary deformation is minor in the range, being restricted to northwest-trending high-angle faults, which in many cases probably followed traces of Mesozoic faults. These young brittle faults probably formed during Late Cenozoic strike-slip faulting [Richard, 1993]. Older, early Miocene extensional deformation, marked by detachment faults and tilted Tertiary strata but no mylonitic rocks, affected the northeastern margin of the Moon Mountains, immediately north of the Dome Rock Mountains, and the southwestern margin of the southern Dome Rock Mountains and adjoining Trigo Peaks (Figure 8) [Sherrod and Tosdal, 1991; Knapp, 1989]. K-Ar and $^{40}Ar/^{39}Ar$ ages for biotite indicate that the range had cooled to <~280°C by the

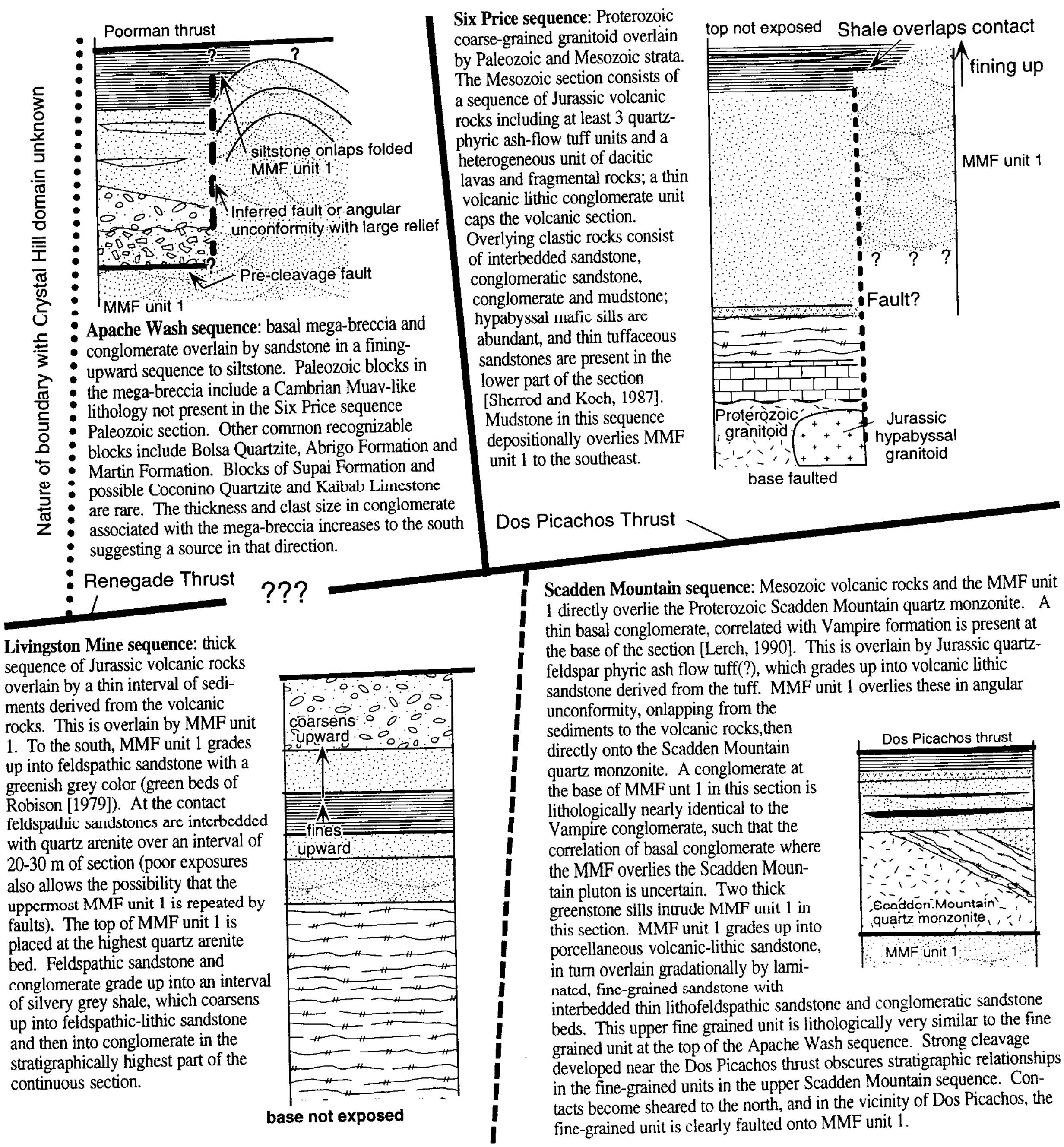

end of the mid-Eocene [Tosdal, 1990; Knapp and Heizler, 1990; S.S. Boettcher, unpublished data, 1993]. Apatite fission track ages, however, suggest that the northern end of the ranges was slightly deeper than the southern end, and cooled to <~100° C in the earliest Miocene, contemporaneous with extensional deformation to the northeast [S.S. Boettcher, unpublished data, 1993]. The thermochronologic data indicate that the range is broadly tilted southward, although the tectonics and magnitude of the tilting are uncertain.

Jurassic plutonic rocks of the Kitt Peak- Trigo Peaks super-unit divide the Dome Rock Mountains into a northern and southern part. The Mesozoic geology of the southern part is described here, and that of the northern part in a following section.

Southern Dome Rock Mountains

In the central Dome Rock Mountains, south of the Middle Jurassic plutonic complex, isolated outcrops of Proterozoic(?) rhyolitic metavolcanic rocks are juxtaposed against a slightly metamorphosed sequence of immature lithofeldspathic clastic rocks and sparse quartzose sandstones (Figure 8). The contact between the two units is poorly exposed or has been modified by younger faulting, but the contact is interpreted as an unconformity because clasts of the rhyolite are present in the metasedimentary rocks near the contact. Where bedding can be discerned, the clastic rocks have steep to vertical dips. The metasedimentary rocks are inferred to be either Late Triassic(?) or Early to Middle Jurassic(?) age, and were deposited across eroded Proterozoic rocks.

The Triassic(?) or Early Jurassic(?) metasedimentary rocks in the central part of the range are in contact with volcanic rocks and intruded by plutonic rocks, both of which represent the Middle Jurassic magmatic arc in the range (Figure 8). Plutonic rocks of the Kitt Peak-Trigo Peaks super-unit intrude the metasedimentary rocks on the north. On the south, they are unconformably overlain by Jurassic volcanic rocks of the Middle Jurassic Dome Rock sequence [Tosdal and others, 1989], which consists of dacitic to rhyolitic tuffs, minor lavas, volcaniclastic rocks, and sparse granitic dikes, sills and hypabyssal plutons. Polyphase ductile deformation and accompanying metamorphism at greenschist facies conditions in the Jurassic(?) and Cretaceous has overprinted most primary volcanic textures. The thickness and homogeneity of the lower part of the sequence suggests that these rock represent caldera-related vent and near-vent facies. On the other hand, rhyolitic tuffs in the upper part of the sequence probably represent out-flow facies.

The southward-dipping Jurassic(?) and Cretaceous McCoy Mountains Formation underlies the southern part of the Dome Rock Mountains. The MMF unconformably overlies the Dome Rock sequence, and overlaps a now-high-angle fault, which juxtaposed two stratigraphic levels in the underlying Dome Rock sequence in the Copper Bottom Pass area (Figure 8). The buried high-angle fault represents brittle late Middle or Late Jurassic(?) deformation. Separation on this fault is consistent with either sinistral strike-slip or normal faulting, which contrasts with the contractional deformation that accompanied plutonism at other times in the late Middle Jurassic in the range [Tosdal, 1990b]. A subtle unconformity separates the upper and lower parts of the MMF in the Dome Rock Mountains. On the eastern side of the range, conglomerate at the base of the upper unit overlies the heterogeneous MMF unit 2, but the base of the upper unit cuts down stratigraphic section to the west, until in the southwesternmost part of the range the upper unit overlies rocks of MMF unit 1 [Tosdal and Stone, 1994].

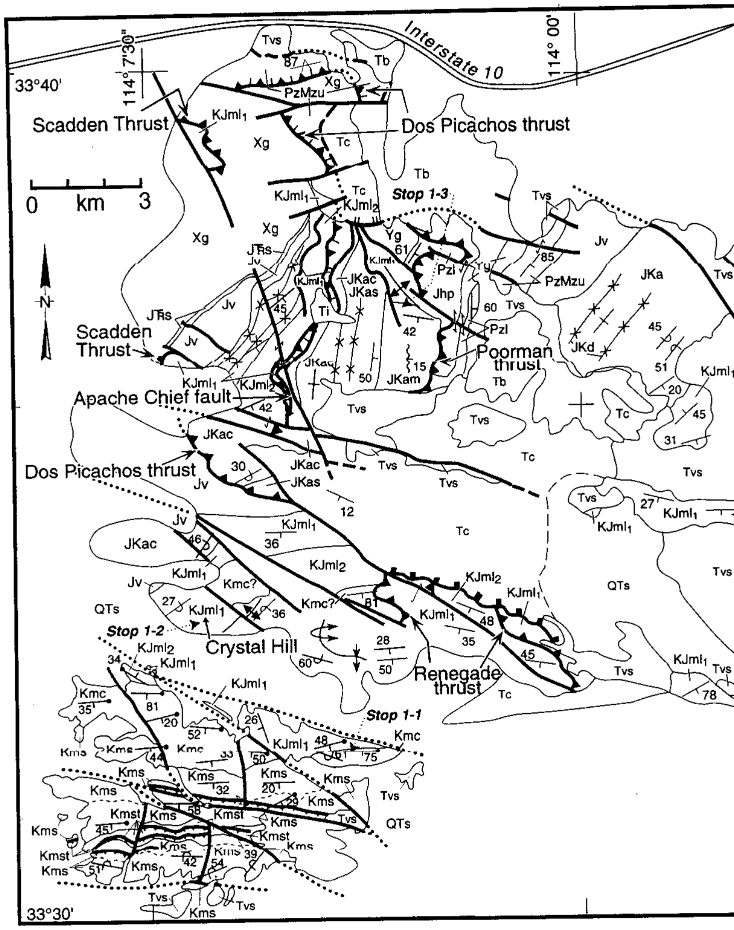

Figure 7. Geologic map of the southern Plomosa Mountains and Livingston Hills, showing location of field trip stops. Modified from Richard and others [1993], Sherrod and others [1990] and Tosdal and Stone [1994]. Explanation of map units included with Figure 8.

In the latest Cretaceous (70±4 Ma) the MMF was tectonically buried beneath the northeast-vergent Mule Mountains thrust system [Tosdal, 1990a], which crops out at the southern end of the Dome Rock Mountains. The upper plate of the Mule Mountains thrust system consists of Middle Jurassic granitoids, identical in age and compositions to those which crop out extensively in the central part of the range.

Northern Dome Rock Mountains (Boettcher)

Overview. Complexly deformed Proterozoic, Paleozoic, and Mesozoic metamorphic rocks are intruded by Middle Jurassic plutons in the central Dome Rock Mountains. Porphyritic granodiorite, the dominant plutonic phase, is mostly weakly foliated to unfoliated, but develops a strong foliation subparallel to its northern contact, where it intrudes a heterogeneous assemblage of Proterozoic metasedimentary and metavolcanic gneisses and megacrystic augen gneiss [Yeats, 1985; Lerch and others, 1991] (Figure 8). Cambrian Tapeats

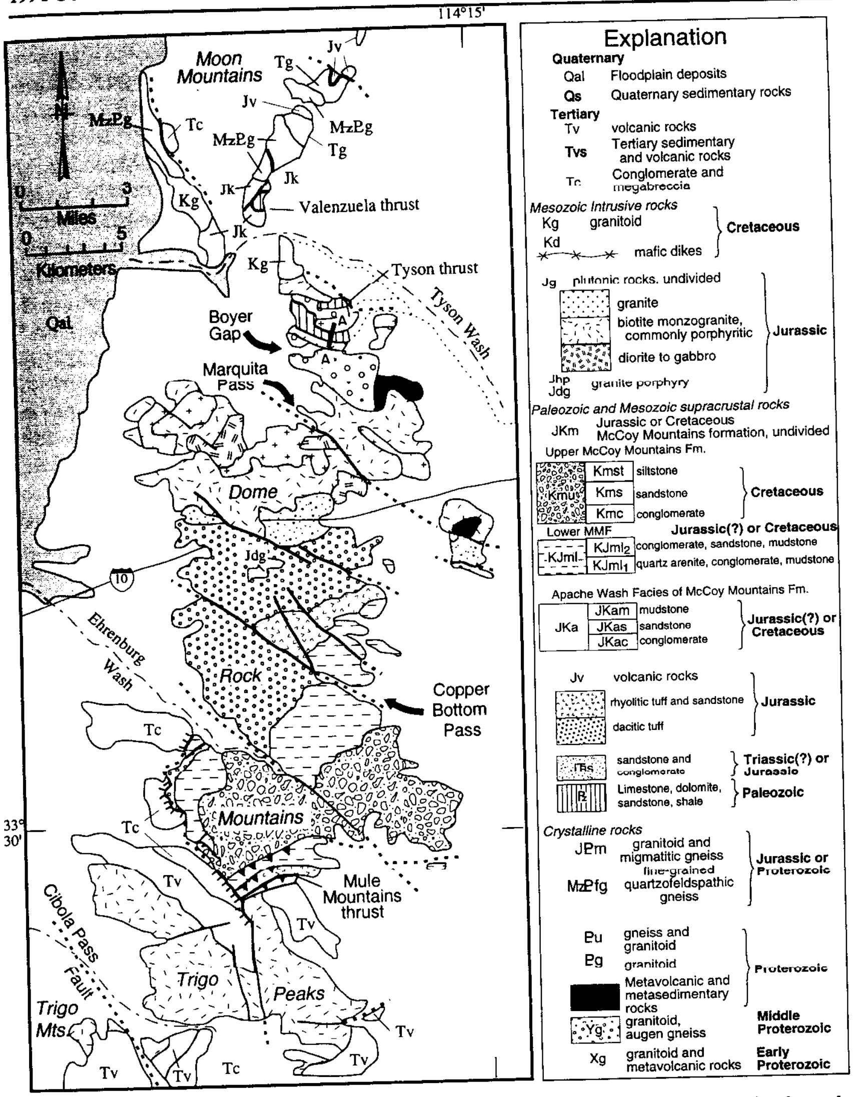

Figure 8. Simplified geologic map of the Dome Rock Mountains showing area of enlarged geologic map of the Boyer Gap area. Modified from Yeats [1985], Knapp [1989], and Stone [1990].

quartzite unconformably overlies the megacrystic augen gneiss in Boyer Gap. A N-dipping mylonite zone on the south side of Boyer Gap (Figure 8) has been interpreted as a regionally extensive shear zone juxtaposing foliated Proterozoic granitoid and overlying Paleozoic metasedimentary rocks on the north against unrelated crystalline rocks to the south [Harding and Coney, 1985; Yeats, 1985]. An alternative hypothesis is that the Boyer Gap shear zone is not a major (>10 km offset) structural boundary, but rather a zone of concentrated shear strain in the footwall of the SW-vergent Tyson thrust shear zone .

Proterozoic augen gneiss, Paleozoic metasedimentary rocks as young as the Supai Group, and Jurassic granitoids in and north of the Boyer Gap area are affected by two phases of Mesozoic contractile (D_1, D_2) and subsequent NE-directed extensional (D_3) strain. Contractile structures lie in the footwall of the Tyson thrust shear zone, exposed 3 km to the north (discussed below). Two kilometers west of the Boyer Gap area the youngest Jurassic granitic phase, a leucocratic, muscovite-bearing granite, is undeformed outside of D_2/D_3 shear zones. The leucogranite intruded as sills parallel to S_1 foliation planes in Jurassic granodiorite gneiss and Cambrian Tapeats Quartzite and is not deformed by a km-scale, north-facing F_1 fold.

The NE-dipping Tung Hill shear zone cuts Proterozoic and Jurassic granitic gneisses; lineation along this zone trends NNE and c/s fabrics indicate top-to-the-NE, normal-sense shear [Yeats, 1985]. Structurally above the Tung Hill shear zone to the north, Triassic(?) metasedimentary rocks (Tung Hill metasedimentary rocks of Yeats [1985]) are in contact with a megacrystic augen gneiss in pendants within Jurassic plutonic rocks. The augen gneiss is lithologically similar to augen gneiss that is depositionally overlain by Cambrian Tapeats quartzite in Boyer Gap.

Mylonitic augen gneiss (~1410 Ma, U/Pb zircon, R.M. Tosdal, unpublished data, 1993) structurally overlies the Tung Hill metasedimentary rocks in the hanging wall of the Tyson thrust shear zone [Yeats, 1985]. Dynamically recrystallized feldspar augen in this shear zone are generally less than 1 cm in diameter and streaks of stretched feldspar are up to 20 cm long, defining a NNE-trending lineation. Winged augen, c/s fabrics, and shear bands show top-to-the-NE, normal-sense shear. The Tyson thrust shear zone is intruded by a late Cretaceous pluton, the Tyson Wash granite (U/Pb zircon, ~80 Ma [R.M. Tosdal, unpublished data, 1993]), at the northern end of the Dome Rock Mountains.

Structures. The earliest recognizable phase of deformation (D_1) produced a N-facing recumbent syncline (F_1) with km-scale amplitude. The F_1 syncline was refolded during a second phase of deformation (D_2) by S- to SW-vergent reclined folds (F_2) with wavelengths of 10's to 100's of meters. The hinge of the F_1 fold crops out ~1 km west of Boyer Gap, where Jurassic and Proterozoic granitic gneiss are folded around Tapeats quartzite and Bright Angel schist. Upward-facing folds are common in Boyer Gap, but at structurally higher levels a 0.5 -10 meter thick section of Cambrian-Mississippian marble is present in the cores of tight 1-10 meter-scale S-vergent synforms above calc-silicate rocks of the Pennsylvanian-Permian Supai Group. The cores of these synforms are inferred to be erosional remnants on the upside-down limb of the F_1 recumbent syncline. Folding of an already upside-down section of metasedimentary rock (F_1 overturned limb) during a subsequent SW-verging phase of deformation (D_2) produced downward-facing folds. Because of the reorientation of D_1 structures during SW-directed D_2 shearing, the initial orientation and vergence of the F_1 syncline is unclear.

D_2 deformation is attributed to top-to-the-SW shearing in the footwall of the Tyson thrust shear zone. Deformation is manifested primarily as SW-vergent isoclinal folds and subordinate ductile shear zones. Compositional layering and a parallel foliation (S_0/S_1) were transposed into a new foliation (S_2) that is axial planar to second generation folds (F_2). Hingelines of minor folds and parallel quartz rods vary from an E-W to a NNE-trend, parallel to the NNE-trending elongation lineation in mylonitic rocks. Brittle, low-angle faults, generally parallel to stratigraphic contacts, locally cut out stratigraphic section and result in both "younger on older" and "older on younger" superposition of metasedimentary rocks.

N-dipping shear zones south of the Tyson thrust shear zone, including the Boyer Gap and Tung Hill shear zones, do not mark pronounced structural or thermal breaks and are interpreted as zones of concentrated strain in the footwall of the Tyson thrust shear zone. In the Boyer Gap shear zone, the mylonitic foliation is folded and transected by a gently (<20°) N-dipping cleavage, producing a subhorizontal intersection lineation. Lithologically similar Proterozoic augen gneiss is present on both sides of the shear zone, suggesting that displacement on the Boyer Gap shear zone is relatively small (<<1 km?). Displacement on the Tyson Thrust shear zone may be as little as a few meters to 1.5 km, the range of thickness of Paleozoic metasedimentary rocks cut out along the fault.

D_3 in the Boyer Gap area is distinguished by open to tight sheath folds that fold quartz rods oriented parallel to F_2 fold axes. These non-cylindrical folds universally show a "z-asymmetry" when viewed looking to the west and generally have sub-horizontal to south-dipping axial planes. Their geometry suggests top-to-the- NE shearing, superposed on the two earlier phases of folding. Additionally, a N-dipping extensional crenulation cleavage in the Tung Hill metasedimentary rocks indicates late top-to-the-NE shearing. Noncylindrical folds of D_2 mylonitic foliation and top-to-the-NE, (normal-sense) shear indicators in N-dipping shear zones are interpreted to be the result of NE-directed extensional strain in reactivated, previously SW-vergent shear zones. Mylonitic foliation with top-to-the-NE S/C fabric, developed in the Tyson Wash granite and related plutonic rocks in the Moon Mountains is probably also related to this deformation. Biotite 40Ar/39Ar cooling ages from the northern Dome Rock Mountains and Moon Mountains are all in the range of 47-56 Ma, indicating that rocks in the area were below ~280°C by early Tertiary time [Knapp and Heizler, 1990] and were too cool to develop mylonitic foliation in early Miocene time. In addition, early Miocene plutons in the NE Moon Mountains are weakly foliated to unfoliated and cut all foliation in surrounding rocks [Knapp, 1989] (Figure 8). Thus, the D_3 extensional deformation is probably Late Cretaceous to early Tertiary in age.

The preservation of strain features (deformation bands and core/mantle structure) in quartz grains, c/s fabrics in D_3 mylonitic rocks, and the progression from ductile to brittle deformation of feldspar implies that NE-vergent extensional deformation occurred under retrograde conditions. The common NE-SW elongation direction shared by D_2 and D_3 deformation phases suggests a possible kinematic link between contraction and extension. As contractile deformation ceased, continued advective heat transfer by water-rich fluids may have provided the trigger that led to gravitational collapse of mid-crustal rocks along preexisting planar and linear anisotropy [Ballard, 1990].

Big Maria Mountains (Hamilton)

The Big Maria Mountains have the most extensive exposures in southeastern California, southwestern Arizona, or northwestern Sonora of the metamorphosed cratonic section of Paleozoic and Lower Mesozoic strata [Hamilton, 1982, 1984, 1987] (Figure 2). The range is dominated by a northwest-trending, recumbently cross-folded synclinorium, flanked by the granitic (~1400 Ma, U/Pb zircon, L. T. Silver, oral communication) and gneissic basement rocks on which the Paleozoic strata were deposited (Figure 9). Middle Jurassic granodiorite and quartz monzonite (~160 Ma, U/Pb zircon , L. T. Silver, oral communication) intrude all older rocks and are present on both sides of the synclinorium. Late Cretaceous regional metamorphism at upper greenschist to middle amphibolite facies was accompanied by intense northeast-verging deformation and attenuation. The thickness of deformed stratigraphic units is extremely variable, locally <1% of initial stratigraphic thicknesses, and yet the distinctive units commonly maintain continuity and stratigraphic position. Voluminous pegmatites with a preliminary minimum age of 63 Ma (U/Pb zircon; J. D. Walker, oral communication, 1993) postdate most deformation, but as pegmatite abundance defines the same general pattern as the thermal contours of the metamorphism the pegmatites and metamorphism reflect the same heat source.

The synclinorium may have formed

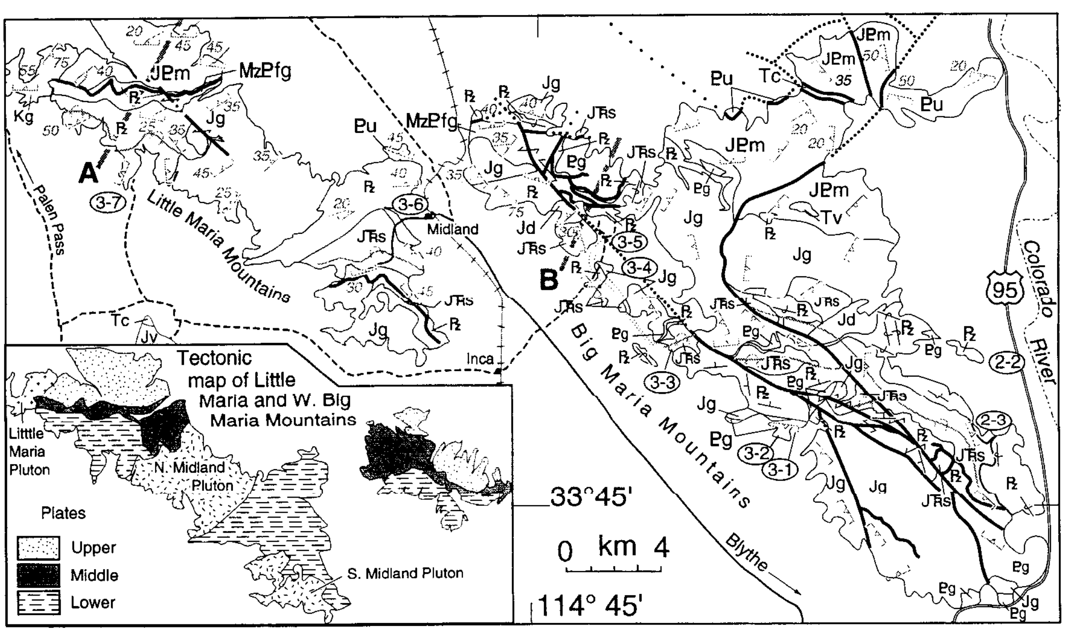

Figure 9. Geologic map of Big and Little Maria mountains. Geology from Hamilton [1987], Ballard [1990], and Stone [1990]. Explanation of map units included with Figure 8.

initially between domiform Jurassic plutons, and Jurassic contact metamorphism survives locally as skarns; otherwise, Jurassic structures and metamorphism were overprinted so severely during Late Cretaceous time as to be unrecognizable. Minor folds in metamorphosed stratified rocks, and c/s fabrics in mylonitic gneisses, show northeastward vergence throughout the range, regardless of their position in the synclinorium or other large structures. Typical mid-size structures are recumbent folds that cascade northeastward over one another. Apparently the metasedimentary rocks dipped steeply when Late Cretaceous deformation began; vergence is shown by structural geometry, not by facing directions of strata within folds. Dips are mostly gentle to moderate to either northeast or southwest; axial planes separating these contrasted dip domains are subhorizontal.

A remarkable feature of the Big Maria Mountains is the extreme tectonic attenuation undergone by the stratified rocks while maintaining stratigraphic coherence. The unmetamorphosed Paleozoic section is about 1 km thick in the Plomosa Mountains [Miller, 1970], whereas in the Big Maria Mountains, the entire section was locally attenuated tectonically to 20 m, with all formations continuous and in proper order (stop 3-3b). Elsewhere in the range, individual units are even more attenuated; Aztec Quartzite and Redwall Marble each maintains continuity where as thin as 30 cm. Such variations are demonstrable here because the undeformed units were so distinctive. Presumably similar deformation is common in metasedimentary terranes but commonly is overlooked.

Early Miocene extension produced a variety of structures in the Big Maria Mountains. A major low-angle normal fault dips northward in the northern part of the range, atop a mylonitic carapace formed early in the extensional episode. Subhorizontal shear zones are present to the south at deeper structural levels. A large moderate-dip normal fault cuts through the range. A thoroughgoing, northwest-trending right-lateral strike-slip fault post-dates early Miocene(?) detachment faulting.

Cooling History (Hoisch). Hornblende, muscovite and biotite from the west-central part of the Big Maria Mountains have yielded $^{40}Ar/^{39}Ar$ plateau dates of 75, 58 and 55 Ma respectively [Hoisch and others, 1988]. The samples were collected within the diopside-tremolite zone, in which the peak metamorphic temperature roughly coincides with the Ar-closure temperature for hornblende. Thus, the 75 Ma cooling age from hornblende is probably close to the time of peak metamorphism. Five K-Ar biotite cooling dates ranging from 52 to 159 Ma have been reported from the Big Maria Mountains and one date of ~60 Ma in the Little Maria Mountains (Martin and others [1982]; data from samples for which >50% radiogenic argon was analyzed and biotite analysis reported >6% K_2O). Most of the biotite K-Ar dates cluster between 52 and 62 Ma, consistent with the $^{40}Ar/^{39}Ar$ plateau age. The cooling data indicate a cooling rate of about 10°C/Ma, much too slow to be accounted for by crystallization of underlying plutons. The relatively slow cooling rate, and gradual changes in metamorphic grade across the range probably reflect either slow uplift or *in situ* relaxation of a perturbed geotherm. A thermal perturbation could have arisen from hot fluid migrating upward through the crust [Hoisch and Hamilton, 1990; Hoisch, 1991].

Little Maria Mountains (Ballard)

Similarities in structural style and in metamorphic grade indicate the geology between the Little Maria and Big Maria Mountains continues without a major structural discontinuity (Figure 9). Structure and rock fabrics in the Little Maria Mountains record at least two episodes of Mesozoic, ductile SE- to SSW-vergent shortening (D_1, D_2), followed by top-to-the-NE low-angle normal shearing (D_3). Field evidence for the early deformation event (D_1) is limited to NE-SW striking large-scale fold limbs and folded, NW-plunging stretching lineation. The younger contractional deformation (D_2) is characterized by large SSW-facing, synformal isoclinal folds, minor SSW-vergent thrust faults, L-S to L tectonite fabric (terminology of Flinn [1965]), transposed intrusive contacts, and extreme amounts of ductile attenuation in the inverted portions of the Paleozoic section. This event was accompanied by upper greenschist to lower amphibolite grade metamorphism (450-600°C) at crustal depths suggested to be 10-12 km in a hot, water-rich, prograde metamorphic environment [Hoisch, 1985, 1987a] (see Metamorphism, below). D_2 contraction was followed quickly by a latest Cretaceous-early Tertiary phase of extension (D_3). Extension decapitated D_2 structures, reactivated D_2 shear zones, and left a legacy of top-to-the-northeast, normal-shear-sense indicators. Structural evidence and the cooling history of rocks in the Little Maria Mountains suggests that extension represents tectonic denudation and gravitational collapse of the D_2 contractional orogen.

The Little Maria Mountains consist of three NE-dipping structural plates (Figure 9, 14), and a relatively undeformed Late Cretaceous pluton at the western end of the range. The lower plate consists of Paleozoic and lower Mesozoic rocks (lithology described in Figure 2) deformed into large, SSW-facing, tight to isoclinal synclines. The middle plate overlies the lower plate above a NNE-dipping tectonic contact and is composed of quartz-rich, grey-green gneiss and muscovite-biotite schist; some Jurassic granitoid is also present. The bulk composition of middle plate gneisses suggests that their protolith was lower Mesozoic sedimentary rocks. A thin layer of transposed Paleozoic marbles overlain by Bright Angel schist and Tapeats quartzite at the top of the middle plate suggests that the contact between the middle and upper plates is an inverted, highly sheared Paleozoic section. Proterozoic or Jurassic feldspathic gneiss and mylonitized Jurassic granodiorite comprise the uppermost plate. Foliation in the gneiss is commonly folded into SSW-vergent antiforms, and intrusive contacts with Jurassic(?) plutonic rocks are transposed into parallelism with the NE-dipping foliation.

Large, mostly granodioritic middle Jurassic plutons intrude rocks within the lower and middle plates in the central part of the range (north Midland pluton) and at the southeast end of the range (south Midland pluton). Large bodies of Jurassic(?) granitoid are present in the upper plate. Intrusive contacts mostly are transposed into parallelism with the main D_2 foliation. D_2 (and possibly D_1) strain transformed the granodiorites into L-S to transitional-L fabric mylonites with stretching lineations plunging to the NE.

Structure. The large-scale fold hinges trend WNW along outcrop strike of the range and plunge gently to the W. The lower limbs of large folds contain abundant small- to meso-scale disharmonic folds, but the stratigraphic sequence is upright and the thickness of units is comparable to that in less deformed sections to the east or north. The upper limbs are inverted and commonly show extreme amounts of ductile attenuation, locally to 5-10% of lower limb thickness. Strain is remarkably homogeneous in these lithologically heterogeneous rocks—each stratigraphic unit, regardless of lithology, is present in correct stratigraphic order and is attenuated by a similar amount. Minor fold axes show a scatter in orientation. Within D_2/D_3 and D_3 shear zones, minor folds are commonly rotated into reclined positions and plunge N to NE, subparallel to the mylonitic lineation, suggesting a sheath fold origin.

D_2 mylonitic fabric is penetrative on the scale of a mountain range. The only D_2 shear-sense indicators remaining in the rock are asymmetric pressure shadows (winged augen), but these are rarely interpretable because of overprinting by D_3 strain. Quartz grains in thin section commonly surround small mica flakes, have a weak undulatory extinction, and a weak or absent preferred orientation. Grain boundaries are not polygonal as would be expected for statically annealed grains but are commonly serrated. Marin [1993] interpreted similar fabrics in the Granite Wash Mountains as indicating highly mobile grain boundaries in a water-rich environment.

An important, late-stage top-to-the-northeast shearing event, D_3, followed soon after contraction ended. In both the lower plate-middle plate and the middle plate-upper plate contacts, mesoscale structures including NE-vergent folds with SW-dipping axial planar fabrics, refolded folds, rotated fold hinges, and asymmetric boudinage are superposed on D_2 fabrics. Hansen separation-arc analysis of small-scale folds in the middle plate-upper plate contact zone in the western Big Maria Mountains demonstrates that the last period of movement along the contact was normal, down-to-the-NE shear. Throughout the area, microstructures in discrete D_3 shear zones uniformly indicate top-to-the-northeast shear. D_3 fabrics are not as penetrative in the rocks as are D_2 fabrics (see below). In the main, they are restricted to D_2 shear zones that were reactivated by D_3 shear or to first generation D_3 shear zones such as the lower plate-middle plate contact.

In the western Little Maria Mountains, the three structural plates can be understood in the context of a single, large SSW-vergent syncline prior to D_3 extension. This interpretation suggests the Mesozoic(?) metasedimentary rocks of the middle plate represent the core of the syncline after translation down dip along a NE-dipping, D_3 shear zone. The lower plate-middle plate contact is interpreted as an inverted, extensively attenuated upper limb of the lower plate syncline. The middle plate-upper plate contact similarly originated as an overturned basement-cover contact in the overturned limb of this fold. Both have been strongly overprinted by D_3 top-to-the-northeast shearing.

D_3 mylonites contain a variety of microstructures reflecting relatively unrecovered crystal plastic strain in quartz, including internal strain shadows, C/S band fabric, quartz shape fabrics, and a strong preferred orientation. Significant grain size reduction has occurred in more intensely foliated zones. These features indicate that the rocks was deformed at temperatures than 300-350°C [Simpson, 1985]. D_3 fabrics formed under vastly different conditions than D_2 fabrics. The rocks were did not remain at high temperatures to be statically annealed; D_3 fabrics were "frozen" into the rock during a rapid retrograde, cooling path.

Interpretation. D_2 crustal contraction was profound and was accompanied by prograde metamorphism, large amounts of water in the crust, high temperatures, and strain rates estimated at 10^{-13} - 10^{-14} sec^{-1}. Geologic evidence from the Little Maria Mountains area suggests that heat was advectively transferred from the lower crust by ascending crustal fluids [Hoisch, 1991]. As a result of this advective heat flow, rocks reached T_{max} in the final stages or very soon after contraction ended at ~80 Ma. Ductile extensional shear zones (D_3) may have become active shortly after this time. Thermochronologic data summarized earlier (Cooling history section, Big Maria Mountains) indicate that the Big Maria and Little Maria Mountains were cooled to below the Ar closure temperature for biotite (~280° C) [Harrison and others, 1985] by 50 Ma. Because microstructures in D_3 tectonites indicate deformation at temperatures above about 300°C, these cooling ages bracket D_3 deformation to be Latest Cretaceous or early Tertiary in age. Contraction and late-stage extension in an orogen are linked through a combination of inherited geometry and thermal history. Calculated slip-line directions for D_2 and D_3 upper plate transport show transport directions nearly 180° apart, suggesting a strong kinematic link as well. Once established, a dynamic/kinematic link may be passed from one orogenic event to another.

METAMORPHISM IN THE NORTHWESTERN MARIA BELT

Boyer Gap area (Boettcher). Two distinct metamorphic mineral assemblages (M_1, M_2) can be documented in the Boyer Gap area. Relict idioblastic tourmaline and kyanite that grew across a schistosity (S_1) preserve the evidence for M1. Tourmaline is present in Proterozoic gneiss, the Tapeats quartzite, in Jurassic metagranite, and in quartzites of the Tung Hill metasedimentary rocks. Kyanite is present in quartz-mica schists of the Tung Hill metasedimentary rocks. The second metamorphic assemblage (M_2) formed under upper greenschist-lower amphibolite facies conditions and is distinguished from M_1 by the growth of metamorphic minerals parallel to a foliation (S_2) that is axial planar to SW-vergent folds (F_2). The assemblage is characterized by quartz+ epidote+ muscovite+ biotite in pelitic schists, quartz+ calcite+ epidote+ diopside+ phlogopite+ microcline in calc-silicate schists and gneisses, and calcite+ muscovite+ quartz +epidote+ actinolite+ phlogopite in marbles. M_1 kyanite is partially replaced by muscovite. Both tourmaline and kyanite were folded, boudinaged, and transposed into the S_2 foliation during D_2. M_2 biotite and phlogopite are partially replaced by chlorite in marbles and schists. Randomly oriented andalusite porphyroblasts overgrow S_2 in pelitic schist of the Tung Hill metasedimentary rocks, indicating that metamorphic recrystallization outlasted D_2 deformation. Furthermore, numerous small (1 m^2) to large (100's m^2) bodies of calc-silicate hornfels and granofels are present at schist/marble contacts and within calc-silicate rocks of the Supai Group in the Boyer Gap area. These bodies are typically found as boudins and consist of very-fine grained, dense, light-tan- to black-weathering calcite- epidote-quartz dominated hornfels and granofels. Irregularly shaped patches of coarse calcite rhombs and biotite are common in calc-silicate granofels and schist. Other minerals recognized in hand sample and thin section include randomly oriented tremolite, microcline, plagioclase, diopside, grossular, and magnetite.

Big and Little Maria Mountains (Hoisch, Ballard). Rocks in the Big and Little Maria Mountains were deformed in a prograde, upper greenschist-lower amphibolite metamorphic environment [Hoisch, 1985, 1987b] at crustal depths suggested to be 10-12 km. Temperatures across the area varied from 400-600 °C with temperature maxima centered over the Late Cretaceous age (?) Little Maria Pluton in the western Little Maria Mountains and over a dike swarm in the western Big Maria Mountains. Variations in metamorphic grade in siliceous metadolomite in the Big and Little Maria Mountains were

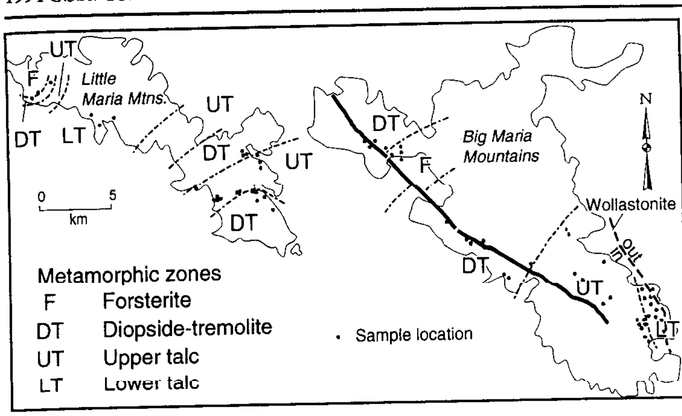

Figure 10. Metamorphic zones in Big and Little Maria mountains.

determined from mineral assemblages, from which four metamorphic zones were delineated (Figure 10) [see discussion in Hoisch and others, 1988]. The zones are the lower talc zone, upper talc zone, diopside-tremolite zone, and forsterite zone. In this area these correspond roughly to upper greenschist to middle amphibolite facies.

Temperatures of metamorphism were determined using the calcite-dolomite geothermometer of Rice [1977]. Temperatures in the Big Maria Mountains range from 428°C to 592°C, and in the Little Maria Mountains from 486°C to 591°C (uncertainty ±50°C). The temperatures determined corroborate the differences in grade inferred from mineral assemblages. In the Big Maria Mountains, metamorphic grade increases gradually from southeast to northwest. In the Little Maria Mountains the highest grade is observed in the contact aureole of the Little Maria pluton at the northwest end of the range. Metamorphic grade varies symmetrically around the hinge of the Midland syncline. The limbs record higher peak temperatures than the hinge, suggesting that the peak of metamorphism was reached prior to folding.

Insight into the pressures of metamorphism may be obtained from the presence of kyanite in the southeastern part of the Big Maria Mountains, where peak temperatures are calculated to have been about 470°C. At these temperatures, kyanite is stable above 3 kbar [Holdaway, 1971]. Hoisch and others [1988] crudely calibrated a geobarometer based upon the anorthite content of albite in plagioclase which has undergone exsolution about the peristerite gap. Plagioclase compositional data compiled from suitable samples corresponds to pressures of 3-4 kbar for samples from the southern Big Maria Mountains and 2 kbar from the southern Little Maria Mountains. Large and unquantifiable uncertainties accompany these estimates. Taken together, these data indicate low crustal pressures, slightly greater than 3.0 kbar in the Big Maria Mountains, and somewhat less in the Little Maria Mountains.

The metamorphism required the flux of an enormous volume of hot H_2O-rich fluid, indicated by the reaction of siliceous limestone in Supai and Kaibab formations to form massive wollastonite [Hoisch, 1987; Hoisch and others, 1988]. Reaction progress calculations [Hoisch, 1987a] show that the reaction requires a water:rock ratio greater than 17:1. The mechanical behavior of the rocks also reflect the same environmental conditions for deformation. Widely varying rock types in the Paleozoic section on the overturned limbs of folds are homogeneously attenuated to 1-10% their initial thickness without indication of significant competency contrast [Hamilton, 1982; Ballard, 1990]. Experimental and theoretical data indicate that such extreme attenuation could only occur under a fairly narrow range of geologic conditions including: 1) abundant water to hydrolytically weaken quartz and to induce highly mobile grain boundary migration; 2) high temperatures to allow dislocation creep in both quartz and calcite; and 3) strain rates of between 10^{-13} sec^{-1} and 10^{-15} sec^{-1} [Ballard, 1990]. The fluid is inferred to have originated from metamorphic devolatilization of subducted oceanic lithosphere and overlying oceanic sediments, which were being subducted at a low angle under the continent at the time of metamorphism [Hoisch and Hamilton, 1990]. Such fluids may have raised crustal temperatures on the order of 140°C at the level of the Big Maria Mountains [Hoisch, 1991].

Road Log

All distances measured in miles.

DAY ONE

0.0 Reset odometer at the intersection of U.S. 95 and Business I-10 in downtown Quartzsite (at the light). HEAD SOUTH on U. S. route 95, between the Dome Rock (west side) and southern Plomosa (east side) Mountains.

8.9 TURN LEFT (mile post 95.5 on U.S. 95); sign on right side indicates 'Kofa Game Range, Crystal Hill.

14.7 Fork, KEEP LEFT on main road.

14.8 Pass left turn to Crystal Hill campground (Kofa Game Range (KGR) signpost #77).

15.5 Pass left turn into Crystal Hill campground (KGR signpost #7).

17.7 TURN off main road on private road to Livingston Ranch. Park on flat area before first wash crossing.

Stop 1-1. Unconformity between lower and upper McCoy Mountains Formation (Tosdal). Walk south approximately 1 mile, aiming for low hills at the northwest end of the first ridge. Outcrops in the wash at the northwest tip of the hills are maroon very fine-grained sandstone of MMF unit 1. Walk a short distance southeast along the wash, and start south up low, white ridge with white quartzite (also unit 1 of the MMF) outcrops. The contact into conglomerate of the upper McCoy Mountains formation is found at the break in slope along the steep north flank of the east-trending ridge (Figure 11). The granite-clast conglomerate is interpreted as equivalent to rocks in the upper part of the upper MMF conglomerate cropping out along strike to the west in the main part of the Livingston Hills. Sparse channels and graded beds indicate that the conglomerate faces southward. The rocks of basal sandstone member 1 dip 40° to 65° southward and are truncated at the contact. A 2-m-thick (or thinner) horizon of maroon mudstone-chip breccia or quartz arenite-clast breccia, both with a purple sericitic matrix, are present along the contact. Angular quartz arenite and sparse maroon mudstone chips are present in the granite-clast conglomerate. Rare bedding in the otherwise massive conglomerate (clast-rich horizons, crude clast imbrication, lenticular grain size variations, and rare interbeds of quartz arenite-clast breccia) indicates that the rocks dip 60° to 90° southward and locally are overturned to the north. The conglomerate beds lie subparallel to the contact. As much as 3 km of stratigraphic section is missing across the unconformity. The missing section is equivalent to an unknown portion of MMF unit 1, MMF unit 2, and the lower part of the conglomerate at the base of the upper MMF.

Return to vehicles, and head back to the west on the main road.

19.9 TURN RIGHT into Crystal Hill campground (KGR signpost #7).

20.2 Windmill at 12-mile well on the right.

20.4 TURN RIGHT at cross roads.

20.5 PARK where road meet major wash (French creek) and curves to parallel wash.

Stop 1-2. Crystal Hill: overturned lower MMF and view of Dome Rock Mountains (Richard, Tosdal). Cross wash and traverse east along bold outcrops of very-fine grained sandstone of unit one of MMF (Figure 11). The outcrops are moderately to strongly cleaved, and have a grey color typical of slightly metamorphosed rocks in this unit. Quartz veins in this area have yielded abundant very clear quartz crystals, thus Crystal Hill and Quartz-Site. The veins typically cut quartzite beds, perpendicular to the bedding, and pinch out rapidly in adjacent fine-grained units. Occasionally the veins are buckled in the fine-grained units before they completely disappear, and the prominent cleavage is axial planar to these folds, suggesting that the veins are pre- or syn-cleavage. Similar veins, present in rock units throughout the southern Plomosa Mountains, generally trend northwest with steep dips and locally contain minor copper mineralization. At the east end of the bold outcrops along the wash, climb out of the wash heading north and look for the trail that heads north towards the saddle between Crystal Hill (the higher hill on the east) and the low hill adjacent to the wash. Follow the trail to the saddle, and climb Crystal Hill, angling up to the north to intersect the prominent quartzite ledge that forms the ridge line. Well developed trough cross beds can be found in this unit that demonstrate that this section is overturned. Follow this sandstone unit to the top of the hill.

From the top of Crystal Hill, looking northwest, the section of overturned lower MMF probably continues under cover at least as far as the low hills in the basin between Crystal Hill and the next high ridge. If this is a continuous section, approximately 830 m of strata are present. Looking east, the south-dipping strata on the ridge about 2 miles away are upright strata of MMF unit 1 above the hinge surface of the large-scale, non-cylindrical, nearly recumbent fold which overturns the strata at Crystal Hill. The hinge is difficult to see in the lower part of the ridge from this angle. Overturned strata of the lower limb are refolded into an upright, NE-trending antiformal syncline in the low hills between Crystal Hill and the upright limb. To the NE of Crystal Hill is a brown hill with no apparent bedding, underlain by boulder conglomerate that probably correlates with the polymict conglomerate seen in the Livingston Hills. This conglomerate unconformably overlies the overturned limb of the Crystal Hill fold, in a relationship similar to that seen along the north side of the Livingston Hills, but with a gently dipping, instead of vertical, unconformity. The conglomerate appears to be folded by the NE-trending F_2 fold. The prominent cleavage in these rocks transects the F_2 fold and the unconformity, demonstrating that it is not related to either generation of folds.

To the south is the north-facing scarp of the Livingston Hills, which are underlain by westward thickening conglomerate of the upper MMF. At the NW tip of the Livingston Hills, upright and south-facing conglomerate and minor sandstone at the base of the upper unit is in contact with an isolated and upright section of rocks assigned to unit 2 of the MMF (Figure 7) [Tosdal and Stone, 1994]. The contact between the upper and lower units at this locality is either an angular unconformity (similar to Stop 1-1) or a premetamorphic fault. Conglomerates of the upper MMF in the NW Livingston Hills are separated from those in the NE Livingston Hills by a northwest-striking, largely concealed fault . This fault is interpreted as a thrust fault with northeast-side up (See Livingston Hills section) that was active before and during deposition of the conglomerate.

To the west across La Posa Plain, the Dome Rock Mountains dominate the skyline. At the north end of the visible part of the range, near I-10, isolated outcrops of Proterozoic(?) rhyolitic

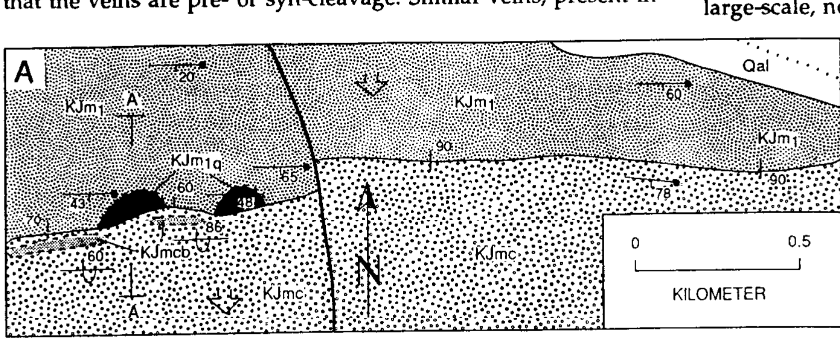

EXPLANATION

Qal Alluvium (Quaternary)

McCoy Mountains Formation of Harding and Coney (1985) (Cretaceous and Jurassic)

Upper unit—

KJmc Conglomerate member—Locally includes:

KJmcb Quartz arenite-clast breccia

Lower unit—

KJm1 Basal sandstone member 1—Locally includes:

KJm1q Quartz arenite

Contact

Fault—Dotted where concealed

Strike and dip of bedding

Strike and dip of overturned bedding

Direction of stratigraphic top

Line of cross section

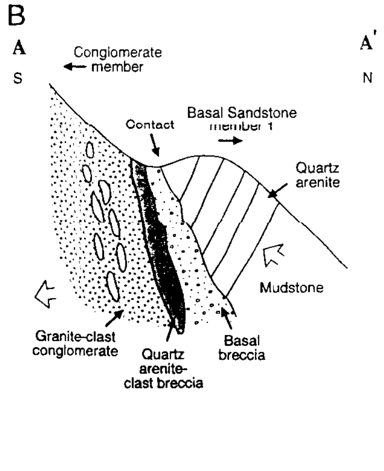

Figure 11. (A) Enlarged geologic map of the northeastern Livingston Hills, southwestern Arizona. See Figure 7 for location. (B) Schematic cross section across unconformable contact between rocks of MMF unit 1 and granite-clast conglomerates in the lower part of the upper McCoy Mountains Formation. Angular truncation of the older rocks at the contact and the subparallelism of conglomerate beds with the contact are emphasized. Cross section is drawn across unconformity at west end of strike ridge shown in **A**.

metavolcanic rocks are overlain unconformably by steeply dipping, Late Triassic(?) or Early Jurassic(?) sedimentary rocks (fig. T4; these rocks form nondescript low hills). Middle Jurassic granitoids intrude the metasedimentary rocks. On the south, SSE-dipping Middle Jurassic volcanic rocks of the Dome Rock sequence are inferred to unconformably overlie the Triassic(?) or Early Jurassic(?) metasedimentary rocks. The sequence is divided into two members, which stand out as lower, massive, and dark-weathering outcrops of dacitic metatuffs, and an overlying, bedded, and light-weathering member of rhyolitic metatuffs and volcaniclastic rocks. The prominent south-dipping strata directly to the west from Crystal Hill are Jurassic(?) and Cretaceous McCoy Mountains Formation. All members of the formation as defined by Harding and Coney [1985] are visible from Crystal Hill. In the section between Copper Bottom Pass and Ehrenberg Wash (bearing 283° to 255° from this vantage), Harding [1982] measured 2350 m of lower McCoy Mountains formation (basal units 1 and 2, and phyllite member), and 3160 m of upper MMF (conglomerate, sandstone and siltstone members). The contact is visible between the silvery, non-resistant phyllite and rugged black conglomerate on the ridge at the edge of the range at about bearing 276°. At the south end of its outcrop, the stratigraphically highest part of the MMF is tectonically overlain by Jurassic metaplutonic rocks along the Mule Mountains thrust system (mostly obscured behind the foreground hill and ridges at the southeast end of the Cunningham Mountain block at bearing 255°). This fault is a shear zone about 1 km thick, dipping 55° to the south, composed of several ductile shear zones and slivers of lower MMF and Jurassic intrusive and extrusive rocks. The South Trigo Peaks, visible at bearing 240°, are underlain by Middle Jurassic plutonic rocks.

Return to vehicles and retrace route to Quartzsite. When leaving Crystal Hill campground, it is quicker to continue straight at first cross-roads (~.1 mile from parking place) to exit the campground at KGR signpost #77 onto main road. HEAD EAST out of Quartzsite and get on I-10 heading east. EXIT FREEWAY at Gold Nugget Road (7.8 miles east of the crossroads in downtown Quartzsite).

0.0 Reset odometer at the top of the off ramp and TURN RIGHT.

0.4 TURN RIGHT on graded dirt road, heading south. The road up Apache Wash is rough and rocky in places; a high clearance vehicle is recommended.

1.4 Fork, KEEP RIGHT and follow wash, skirting outcrops of Scadden Mountain pluton.

1.8 Fork, keep left in the main wash at both this fork and a second one about 50 m further on (second one marked by a cairn).

1.9 Fork, TAKE RIGHT, and climb out of main wash onto old alluvium after about 100 m. Heading south, Dos Picachos will lie directly in front; this is a klippe of Devonian and Mississippian carbonate on Mesozoic sandstone.

2.5 Fork, TAKE LEFT and drop back into the main wash. (right fork heads to the Belle of Arizona mine, and to prospects around Dos Picachos). The tracks in the wash can change depending on recent floods.

2.7 VEER TO LEFT and follow left forks on anastamosing tracks in braided channel. Large boulder in outcrops on the right is block of Jurassic volcanic rock in Tertiary breccia [Davis, 1985]; breccias are well exposed in the east face of hill on the west side of wash south of here. Italian and Apache washes join in this area; the route will follow Apache Wash (the left fork).

3.1 Road leaves prominent channel and climbs slightly onto older alluvium; cairn at intersection.

3.2 CLIMB out of main wash onto old alluvium on east side of Apache Wash.

3.9 Continue straight, dropping into Apache Wash; road from Chalk Wash enters from the left. From here, the route follows Apache Wash along one of several anastamosing tracks in the braided channel.

4.5 Fork, KEEP LEFT in main wash. Right fork goes to Apache Chief Mine.

4.7 Proterozoic granite (depositionally overlain by Cambrian Bolsa Quartzite) is faulted against unit 1 of the MMF in small side canyon on east side of main wash. This high angle fault is overlapped by the Poorman thrust.

5.3 Road works to east across wash, crossing Apache Chief Mine fault. Bold tan outcrops on top of the low ridge on east side of wash are unit 1 MMF quartzite tectonically overlying conglomerate of the Apache Wash facies.

5.7 Follow tracks near the east side of the main wash. Outcrops of highly cleaved siltstone of the Apache Wash facies on the east side of the wash; dark outcrops on the west side of the wash are sandstone of the Apache Wash facies stratigraphically below the siltstone. The fault that juxtaposes the sandstone and siltstone against conglomerate is cut by the Apache Chief Mine fault.

6.0 Wash enters from left (east), on south side of steep hill (basal McCoy Mountains Formation above Apache Chief Mine fault); pass sandstone outcrops in wash bottom along track.

6.1 PARK after passing outcrops in wash, in front of gently dipping well bedded sandstone.

Stop 1-3. Unconformity between siltstone of Apache Wash Facies and basal McCoy Mountains Formation (Richard). Climb hill above sandstone outcrops along wash, heading east (See Richard [1992b] for detailed map). The contact between sandstone and 'siltstone' (fine-grained, very thin-bedded sandstone) of the Apache Wash facies is typically gradational, but structural disruption of bedding, which intensifies near the contact, makes the location of the contact indefinite. Tan outcrops on ridge to north are Paleozoic carbonate blocks in sedimentary breccia at contact between lower McCoy Mountains Formation and fine-grained Apache Wash facies strata. Traverse east along low, hilly ridge crest. The variability of bedding orientations, which is typical of the fine-grained upper part of the Apache Wash section , hinders estimating the true stratigraphic thickness. Continue to the second hill top capped by old alluvium. On the east side of the summit, arkosic grit beds appear interbedded in the fine-grained sandstone. This is the beginning of a rapid gradation (over about 10 m of section) into sedimentary breccia consisting of blocks of lower Paleozoic carbonate and quartzite and Proterozoic coarse-grained granitoid. Continue up ridge to contact with quartz arenite of the lower MMF, and follow the contact into the wash just east of the ridge where it is well exposed. Note that the cleavage in these rocks transects the contact. Red staining and bleaching of McCoy Mountains formation near the contact is interpreted to reflect weathering before deposition of the overlying sediments. Return to the truck, and retrace route to Quartzsite.

DAY TWO

0.0 Reset odometer at intersection of US 95 and Business I-10 in Quartzsite, AZ; Drive north on US 95.

1.6 - TURN LEFT (west) onto Tyson Drive (Fire station on right).

2.3 - TURN RIGHT (north) onto Moon Mountain Road (follow sign to Quartzsite Alliance Church).

5.7 - VEER LEFT at prominent branch in road marked by wooden stake.

6.8 - VEER LEFT at prominent branch in road marked by metal stake. Pass light-colored, low hills on left, underlain by Jurassic granitoid and Paleozoic(?) quartzite, schist and siliceous marble. 9.8 - PARK on right (north) just before entering area of bedrock exposure in Boyer Gap.

Stop 2-1. Large-scale refolded folds in Paleozoic metasediments (Boettcher). From parking area, walk SSW to top of low hill on the south side of the road to view fold structure looking west, approximately along the F_2 hinge trace (Figure 12). This hill is underlain by Bright Angel schist with a crenulated, penetrative schistosity (S_2) that is axial planar to isoclinal folds of compositional layering and parallel schistosity (S_0/S_1). Rodding lineation and striations in quartzite layers within the schist are parallel to F_2 minor fold axes and locally produce L-tectonite fabrics. Non- penetrative, spaced cleavage (S_3) locally transects the earlier fabrics present in the metasedimentary rocks. The gradational contact with Tapeats quartzite is exposed on the south side of the hill. The Tapeats quartzite depositionally overlies Proterozoic coarse-grained granite (now variably deformed to augen gneiss). These rocks are located on the upright limb of both F1 and F_2 folds. Looking west at the steep hill on the north side of Boyer Gap, note the two tight synforms of light colored, lower Paleozoic marble within the darker Supai formation. These synformal anticlines are interpreted as the cores of F_2 minor folds on the overturned limb of a N-facing, km-scale F_1 fold. This outcrop is near the core of a larger (wavelength of 100's of meters) F_2 fold. Walk northwest across the road, crossing into Cambrian-Mississippian marbles and then into Supai Formation calc-silicate schists and gneisses. Lenses of calc-silicate rock in the marble below the contact with the Supai Formation may represent infolding of Supai Formation with the marble, or may represent fluid channelways along which the marble has been metasomatized. Traverse west along the base of a steep outcrop of complexly folded lower Paleozoic marble and climb up along the west side of this cliff, working up the hill back into Supai Formation rocks, and finally to the hinge zone of the lower of the two synforms preserved near the hill top. Return to vehicles by the same route.

Optional Stop 2-1a. Tung Hill metasedimentary rocks (Boettcher). Return to vehicles and retrace route back to Quartzsite.

14.8-(mile 6.8 inbound)TURN SHARPLY NORTH on dirt road marked by metal stake at mile.

16.4-VEER LEFT.

16.8-Veer left.

17.1-Veer left.

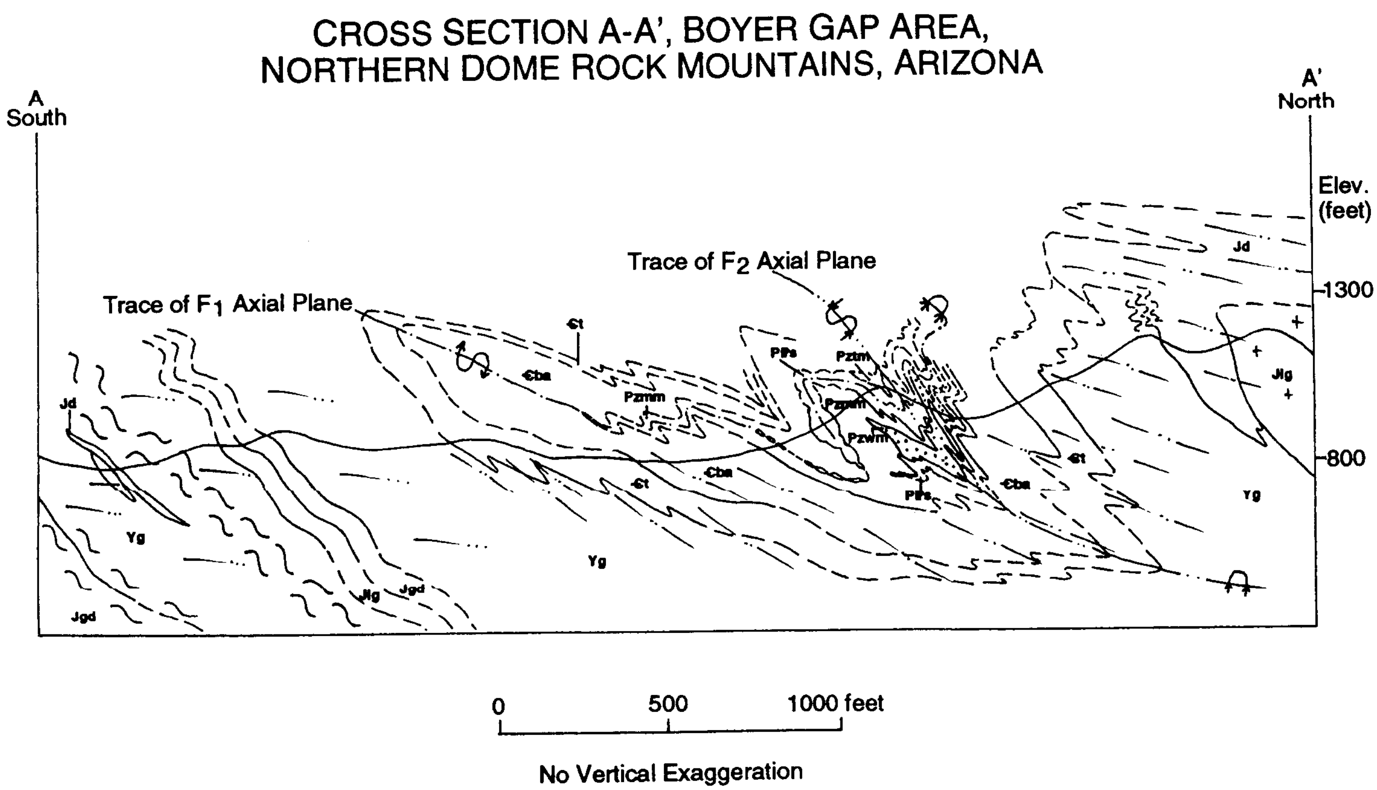

Figure 12. Detailed cross section of Boyer Gap area, by S. Boettcher. Section line shown in Figure 8. Abbreviations for map units (alphabetic order): Cba-Bright Angel schist (Cambrian), Ct-Tapeats quartzite (Cambrian), Jd-diorite (Jurassic), Jgd-granodiorite (Jurassic), Jlg-granite (Jurassic), PPs-Supai formation (Pennsylvanian-Permian), Pzmm-mottled marble (Cambrian to Mississippian), Pztm-tan marble (Cambrian to Mississippian), Pzwm-white marble (Cambrian to Mississippian), Yg-coarse-grained granitoid to augen gneiss (Middle Proterozoic).

17.2 Veer right.

18.1-Park on right (north) side of road. Walk north across wash to knobby outcrops of Proterozoic and/or Jurassic protomylonitic augen gneiss that underlie Tung Hill metasedimentary rocks. The metasedimentary rocks consist dominantly of quartz-mica schist, with lesser amounts of quartz-kyanite schist, yellow/tan micaceous marble, quartz-pebble metaconglomerate, and quartzite. These rocks are intruded by Jurassic granitoids and are in contact with Proterozoic or Jurassic augen gneiss, but are nowhere in contact with the Paleozoic metasedimentary rocks at Boyer Gap. A Triassic age has been inferred for this assemblage based on correlation with other early Mesozoic sedimentary rocks present in nearby ranges and with the Moenkopi Formation of the Colorado Plateau [Reynolds and others, 1987; Knapp, 1988]. The lower contact of the metasedimentary rocks with Proterozoic(?) augen gneiss is hypothesized to be depositional in nature, although subsequent deformation obscures this relationship. To view Proterozoic mylonitic augen gneiss in the hanging wall of the Tyson thrust shear zone (described above), walk north ~100 meters around the east side of the low hills until dark weathering mylonitic augen gneiss is reached.

Return to vehicles and retrace route to Quartzsite. Get on Interstate 10 heading west, cross the Colorado River into California, and exit at the U. S. 95 exit on the east side of Blythe (first exit after crossing the river). Reset odometer at the stoplight at the intersection of U.S. Highway 95 and Hobsonway (the main street in Blythe)

00.0 HEAD N on US Highway 95 on the Holocene floodplain of Colorado River. Big Maria Mountains come into view ahead. Dark hills directly ahead are of granitic rocks; layered rocks in left part of range are metamorphosed Paleozoic strata.

4.5 Cross irrigation ditch. Rugged hills ahead and left are of Jurassic granitic rocks; lower hills and dissected pediment to right are of Proterozoic granite. Late Pleistocene fan surfaces are pediments on intercalated fanglomerates and river silts.

6.1 Cross large ditch and begin curving route along edge of floodplain. Wash cobbles for next 3 miles are mostly of Jurassic granitic rocks, with subordinate Proterozoic granites.

7.9 Roadcut in Proterozoic granite, recrystallized at greenschist facies.

11.1 Defunct restaurant on right. Dark Supai Fm at 10 and 11 o'clock; Kaibab Marble and other Permian units at 10:30; lower Paleozoic at 9:30.

11.5 Indian Reservation sign. Supai Fm on left: darkly varnished greenschist-facies calc-silicate and quartzitic rocks, derived from calcareous redbeds. At this low grade, the formation is typically covered by several m of jostled blocks solidly cemented by calcite.

12.4 Near hills at 10 o'clock are of recumbently interfolded dark Supai Fm, cream-colored Redwall Marble, and yellow dolomite marble. Tectonic attenuation is to ~10% of initial thickness.

14.4 Highway rises from floodplain to fan; graded road to W.

16.2 TURN LEFT at track into transformer. **Stop 2-2. View of metamorphosed Paleozoic strata** (Hamilton). Near hills bearing 280°-290° are on NE limb of a synclinorium and display dark Supai Fm, thin gray Redwall Marble, and tan metadolomite, repeated in tight recumbent folds. Cambrian strata and Proterozoic metagranite are present low in frontal hills. A Tertiary normal fault, near side down 1.5 km, intervenes between frontal hills and distant high ridge. High peak at 265° is of Supai Formation with yellow Cambrian-Mississippian carbonates beneath and left, and dark Cambrian clastics and Proterozoic and Jurassic metagranite below those. Above and right of Supai Formation are poorly exposed Hermit Schist and Coconino Quartzite, then cliffs of light Kaibab Marble, then dark Triassic rocks, Aztec Quartzite, and Jurassic metaignimbrite. Skyline at 276° is of inverted Paleozoic section, greatly attenuated tectonically but complete, which is connected to the thick section at 265° by a syncline that is broadly upright although cross-folded by large, tight recumbent folds. Skyline peak at 301° displays a N-verging recumbent fold of a septum of Paleozoic metasedimentary rocks between plutons of Jurassic granitic rocks, now mylonitic gneisses; this is not part of the main synclinorium. Skyline at 310° is below the projection of a middle Tertiary detachment fault that dips north down the far side; the light stripes, concordant to mylonitic foliation, are boudinaged pegmatites of the Late Cretaceous swarm that are undeformed in most of the range and which here may record mid-Tertiary extensional ductile deformation when this terrain was still at mid-crustal depths. Return to vehicles and BACK TRACK south on US 95.

18.0 (mile 14.4 N-bound) TURN WEST on graded dirt road. There may be a chain across the road but in recent years it has been unlocked.

18.45 Pass pile of rip-rap from the quarry at end of this road.

19.35 PARK before iron posts, on east side of major wash. The road is impassable for any but the most determined from here. **Stop 2-3. View of inverted fold limb and outcrops of Triassic(?) strata** (Hamilton). To NW is inverted upper Paleozoic and lower Mesozoic section in NE limb of synclinorium. Structurally highest in sight is dark Supai Fm. Below that are poorly exposed Hermit Schist and Coconino Quartzite, then conspicuous striped Kaibab Marble. Below Kaibab are green Triassic rocks, and below those is reddish Aztec Quartzite, the present tectonized thickness of which decreases greatly between peak at 295° and low knobs at 280°. (Out of sight to left, SE of Stop 2B, thickness decreases to <1 m.) Below Aztec, forming green hills, is Jurassic metaignimbrite. The discontinuous veneer of yellowish-gray algal travertine on the lower hills in the foreground is the basal deposit of the Bouse Fm of early or middle Pliocene age; the lower hills and canyons now being exhumed are of pre-Bouse age. The embayment by which the marginally marine Bouse connected to the sea has not been recognized. The various alluvial-fan levels record a number of Pleistocene exhumation and pedimentation events in response to changing climate, not to local uplift.

Walk along road, crossing the major wash. The peak to the SE has inverted upper Paleozoic section, metamorphosed at upper greenschist facies (calcite and quartz stable): Supai Fm at top, poorly exposed Hermit Schist beneath it, small cliffs of Coconino Quartzite next below, and cliffs of Kaibab marble and cherty marble near bottom. Kaibab Marble on the west side of road shows isoclinal folds refolded by recumbent folds showing overfolding NE down the dip. *The Kaibab has plane-parallel external contacts so fold superpositions are due to combined simple shear and pure-shear flattening, not to superposed compressive deformations.* Continue south on road, past small E-dipping normal fault that drops Triassic or Jurassic metaconglomerate against Kaibab, and enter wash, heading upstream (right). Outcropping metaconglomerate has boulders of Proterozoic granite and Paleozoic units. Granite and quartzite boulders are flattened 1.5-2:1; limestone, now calcite marble, to 50:1. The Paleozoic section is preserved in ranges nearby to W, N, and NE, so the eroded uplift likely was to the S or SE and may have been related to emplacement of Late Triassic granites in the Mule Mountains although no clasts of those granites have been recognized here. A small pluton of schistose mafic Jurassic granodiorite was mostly removed from the quarry to the S. In its northern contact area is dark bluish-gray kyanite quartzite (contact-metasomatized Aztec quartzite(?)), large blocks of which are present in the wash. Cobbles in wash include abundant Jurassic granites, with proportion of felsic rocks increased over that in outcrop. Granodiorite and quartz monzonite are relatively rich in clotted mafic minerals, low in quartz, and characterized by equant lavender K-spar phenocrysts that often have white rims. Alaskite forms irregular masses within the other Jurassic granites. Subordinate cobbles of Proterozoic quartz-rich leucogranite consist mostly of K-spar megacrysts. These rocks retain granitic fabrics despite upper-greenschist recrystallization. Farther NW in the range, amphibolite-facies metamorphism rendered all granites gneissic, but the Jurassic and Proterozoic types are easily distinguished even as mylonitic gneisses. Walk downstream across the road, through inverted Triassic metaconglomerate, epidotic metasediments of lower part of Triassic section, and Kaibab Marble. Kaibab and Triassic show low-temperature mylonitic intershearing, perhaps by mid-Tertiary crustal extension. Farther down wash is Pliocene travertine, with cemented clastic strata that were foreset into standing water, barnacle coquinas, and small to very large algal heads.

Return to vehicles, and drive back to U. S. 95., turn south and return to Blythe. (If you are continuing directly to stops on the west side of the range, turn right (west) on Fourth Ave. (9.8 miles after getting on U.S. 95) and join Day 3 road log at 4.5 miles N of Hobsonway).

DAY THREE

Reset odometer at stop light at the intersection of Hobsonway and Lovekin in Blythe (Lovekin is an exit from I-10 in west-central Blythe).

0.0 HEAD NORTH on Lovekin, which becomes the Midland road upon leaving town.

4.5 Pass Fourth Ave.

5.5 Cross railroad tracks.

8.2 TURN NE off pavement on dirt road at red pipeline marker 290.

12.7 Fork, TAKE RIGHT BRANCH. Pass small rock piles on the left.

13.3 PARK on high fan surface just short of outcrop hills. **Stop 3-1. Upright Paleozoic section in lower amphibolite facies** (Hamilton). WALK E into main wash and then about 200 m N and NW up it. Encounter in outcrop: first foliated Proterozoic metagranite; then, Tapeats Quartzite, with much impure metasandstone in lower part, abundantly folded with NE vergence, and cut by a mid-Tertiary dike. Wash boulders include metamorphosed Jurassic quartz monzonite. CLIMB SW up section, along road until reaching first ridge crest (just after mafic dike) over dark, glossy muscovite-biotite Bright Angel Schist; dip mostly SW. Leave road and continue up ridge to calc-silicate ledge at the top of the Bright Angel. Enter coarse, foliated calcite Muav Marble. Section continues upward (we will not) through cliffs of brown-weathering metadolomite, white Redwall Marble, and dark Supai Fm. All of these units are internally isoclinally folded and externally recumbently folded, but the structure looks simple from here because fold axes are subparallel to cliffs. A small normal fault high in the cliffs puts metadolomite against Supai and truncates a Tertiary dike. Supai wollastonite is prominent in talus. Bulldozer tracks were made for gathering stripey weathered blocks of wollastonitic Supai for decorative facing stone. Interfolded Coconino Quartzite and Kaibab Marble are visible on distant ridge to N. Return to vehicles and BACKTRACK along dirt road.

13.9 TURN RIGHT at rock piles (= 13.3 inbound) and drive NW parallel to mountain front.

14.5 PARK at S end of hill. **Stop 3-2 Jurassic metagranitoids and view of upright Paleozoic metasediments** (Hamilton). Hill consists of Jurassic metagranodiorite (equant K-spars survive as augen) and meta-alaskite. Foliation dips W: this is in overturned limb of a recumbent fold relative to upright NE dips in mountain face. CLIMB HILL for view. Mountain face has dark Supai on thin, white Redwall on yellow-brown dolomite + Muav on (at lower right) dark Cambrian clastics, basement, and Jurassic granite. NE-verging Z fold in cliffs at 342° involves Supai, Redwall, and dolomite. Wollastonite layer high in Supai weathers pink; green Hermit Schist shows locally above Supai at top of mountain. Return to vehicles and RETRACE route to paved Midland road.

19.6 (= 8.2 inbound). TURN RIGHT (northwest) on Midland road.

21.1 Pass entrance to Midland LTVA campground.

23.9 Pass dirt road to NE at phone pole 272620. The entire Paleozoic section can be seen in the NW-trending frontal ridge, as the SW and here upright limb of the main synclinorium of the range. The units are internally isoclinal but superficially appear simple; lithologic layering dips NE, and traces of contacts mostly plunge gently NW along the front of the ridge. The lower units, from Precambrian basement up to Supai Formation and locally Hermit Schist, are exposed to the right of the canyon, NE of here, through the frontal ridge, and were seen at Stops 3-1 and 3-2. The higher units are exposed left of that canyon. Dark cliff-forming Supai Formation, with pink wollastonite layer near top, is overlain by recessive green Hermit calc-silicate schist; next higher is Coconino Quartzite, forming rubbly brown cliffs; and highest is light-colored cliff-forming Kaibab Marble.

25.2 Double-pole power line crosses highway. In frontal ridge to NE, units Kaibab/Coconino/ Hermit/Supai dip progressively to fan level going NW.

26.1 TURN RIGHT (NE) on dirt road.

28.0 PARK for optional stop 3-3a, after passing between hills of dark, wollastonitic Supai Fm. Dip is mostly SW in these low hills because the axis of a recumbent crossfold lies between here and main ridge. Look at main ridge to SSE at thick Paleozoic rocks of S limb of syncline, and to ENE at those of very thin N limb, separated by drab Mesozoic stratified rocks.

29.2 PARK below blasted-out prospect in white wollastonite in N-dipping Kaibab Marble. **Stop 3-3 Attenuated Paleozoic section** (Hamilton). Mesozoic section exposed in peak to north (from top): inverted dark Jurassic metavolcanic rocks (Jv); light-colored Jv (contains axis of main isoclinal syncline), rest of top half of hill; brown Aztec Quartzite; and Triassic metasediments in lower slopes. Undeformed Late Cretaceous pegmatites cut all these rocks. Walk northwest along the east side of the low hill of slightly micaceous Aztec, towards the low saddle between this hill and the high ridge to the north.

Look E to isoclinal interfold of Kaibab and Triassic on main range crest. Continue NW from saddle along the base of the steep slope and up small canyon, through thick Jv to inverted Mesozoic and Paleozoic section, which dips 40° N and is metamorphosed at lower amphibolite facies. *Section is complete despite tectonic attenuation to 2% of stratigraphic thickness.* Outcrop and hand-specimen appearance is not much different from that of sections much less attenuated: layering and grain size are controlled more by syntectonic recrystallization than by initial bedding. Units and present thicknesses, in order going structurally upward and stratigraphically downward: dark Jv, 3 m; Aztec Quartzite, 2 m; green Triassic metaclastic rocks, 2 m; white and buff Kaibab Marble, 3 m; vitreous Coconino Quartzite, 0.5-2 m; gray Hermit Schist, 1 m; dark cliff-forming Supai Fm, 5 m; white Redwall Marble, tectonically intercalated with Supai, 1 m; yellow metadolomite, 5 m; Muav Marble, 2 m; biotitic Bright Angel Schist, 1-2 m; brown Tapeats Quartzite, 2-3 m. Proterozoic metagranite lies above the Tapeats, and Jurassic metagranites still higher; these too must be extremely flattened. Small folds, most obvious in Supai Fm and Jv, plunge WNW parallel to mineral lineation and show NNE vergence. The main synclinorium is isoclinal and its invisible hinge may lie in the light Jv only several meters below dark Jv.

Highly ductile deformation characterizes the "Maria fold and thrust belt" where metamorphosed under amphibolite and upper greenschist conditions. Many of the purported thrust faults in the province represent thermally controlled fronts of ductile deformation or zones in which high strain is made obvious by flattening of stratigraphic units (as at this locality). The term 'thrust fault' has been misapplied where rock continuity was maintained through pervasive but coherent deformation. Return to vehicles and BACKTRACK to Midland Road.

32.2 (= 26.1 inbound) TURN RIGHT (NW) on Midland Road.

34.8 TURN RIGHT on dirt road, opposite graded road and large white rock (road to west is the Inca road, route to stop 3-7).

37.5 PARK after passing hill on right. **Stop 3-4. View of pegmatite swarm** (Hamilton). This is near the center of a great swarm of almost undeformed Late Cretaceous muscovite pegmatites that cut the extremely deformed metamorphic rocks. Dikes decrease upward in high ridge of augen gneiss (Jurassic metagranodiorite) to E. Peraluminous granite likely underlies this area but is not exposed. The highest temperature metamorphism occurred in this area of voluminous pegmatites, so dikes and metamorphism likely reflect related sources of heat and water. High, dark ridge to N displays inverted N-dipping Paleozoic metasediments that intertongue to right into augen gneiss (Jurassic metagranodiorite) because of extreme Cretaceous transposition of a steep Jurassic intrusive contact. On the distant ridge to NE, a septum of Paleozoic metasedimentary rocks dips N between Jurassic augen gneisses; this is the upper limb of the recumbent fold seen at 301° from Stop 1. Return to vehicles and continue travelling N on this road.

38.0 TURN RIGHT at fork.

38.3 VEER RIGHT at fork.

38.4 PARK. **Stop 3-5. View of tectonic stratigraphy in western Maria and Little Maria Mountains** (Ballard). Looking north, the three structural plates that characterize the western Big Maria and Little Maria Mountains can be seen (Figure 13). The lower plate is represented by a small portion of the upper limb of the D_2 Little Maria (Midland) syncline. At this location, the hinge surface trace is in the valley just south of this stop. The middle plate crops out midway up the south-facing slope and consists of quartz-rich gneiss and an upper band of muscovite-biotite schist. The middle plate-upper plate contact is represented by a thin strip of Paleozoic marble with Tapeats Quartzite in the top. *(Hamilton disagrees with this and other interpretations by Ballard).* Return to vehicles and RETRACE route to Midland Road. Reset odometer at Midland road.

0.0 TURN RIGHT (northwest) on Midland road.

3.9 Fork, FOLLOW PAVED ROAD TO RIGHT; dirt road continuing NW is Rice Road.

4.5 Cross railroad tracks, and enter remains of Midland. Follow the paved road. The low, east-trending ridge north of road is an east-striking, nearly vertical section of (from south to north) Proterozoic(?) gneiss, Cambrian-Devonian marbles, and Supai Formation (on the ridge crest). This is one of the only N-facing stratigraphic sequences in this range; poor outcrop obscures the folds or faults that bound it.

5.5 PARK in gap through ridge. **Stop 3-6. View of Midland syncline** (Ballard). Climb low hill to north of road for view to NW of the core of the Midland syncline. The contact between Kaibab marble and Triassic gypsiferous phyllite is poorly exposed in the southwest slope of the hill. The stratigraphy is overturned; Coconino quartzite and then Supai formation are crossed up the hill. Note north to northeast-plunging minor folds, with hinges parallel to rodding lineation in the Coconino quartzite. The northeast-striking upper limb of the Midland syncline on the west side of the basin area west of this hill is vertical. The Supai formation in this limb is intruded on the northwest by Jurassic granitoid in the high ridge bounding the west side of the basin. The syncline has been refolded along a NNE plunging axis, such that the strike of the upper limb swings to northwesterly as the section becomes overturned in these low hills near Midland. In the Midland area several generations of N- and NW-trending lineations have been refolded and overprinted with an NE-plunging lineation. The NE trend of the upper limb of the Midland syncline and the N-NW plunging lineation in the Midland area and in the western Big Maria Mountains just to the west are the only remaining evidence for D1 deformation. Dark-greenish grey Triassic(?) gypsiferous phyllite and calcareous metaclastic rock crop out in the core of the Midland syncline. The lack of marker units and probable diapiric movement of the evaporite units make it impossible to map the hinge of the large-scale fold precisely. Return to vehicles and RETRACE route through Midland along paved road to the Inca Road.

11.0 TURN RIGHT (west) on Inca Road (at large white rock; this is where the odometer was reset en route to stop 3.6). Road mileages to stop 3-7 are approximate.

12.6 Cross railroad tracks, enter ruins of Inca; follow well used track that runs south (parallel to railroad tracks) about .1 mile, then curves to right (west) after passing burned out trailer and building. The northern McCoy Mountains lie directly ahead; the contact between Jurassic volcanic rocks and basal unit one of the MMF is the boundary between massive and bedded rocks at about 11 o'clock.

18.3 Fork, KEEP LEFT. Follow Arlington Mine road westward towards the northern tip of the McCoy Mountains. Track to left just after fork leads to St. John's mine area in the large canyon that drains the middle of the McCoy Mountains. The northern tip of the range is megabreccia derived from Jurassic volcanic rocks.

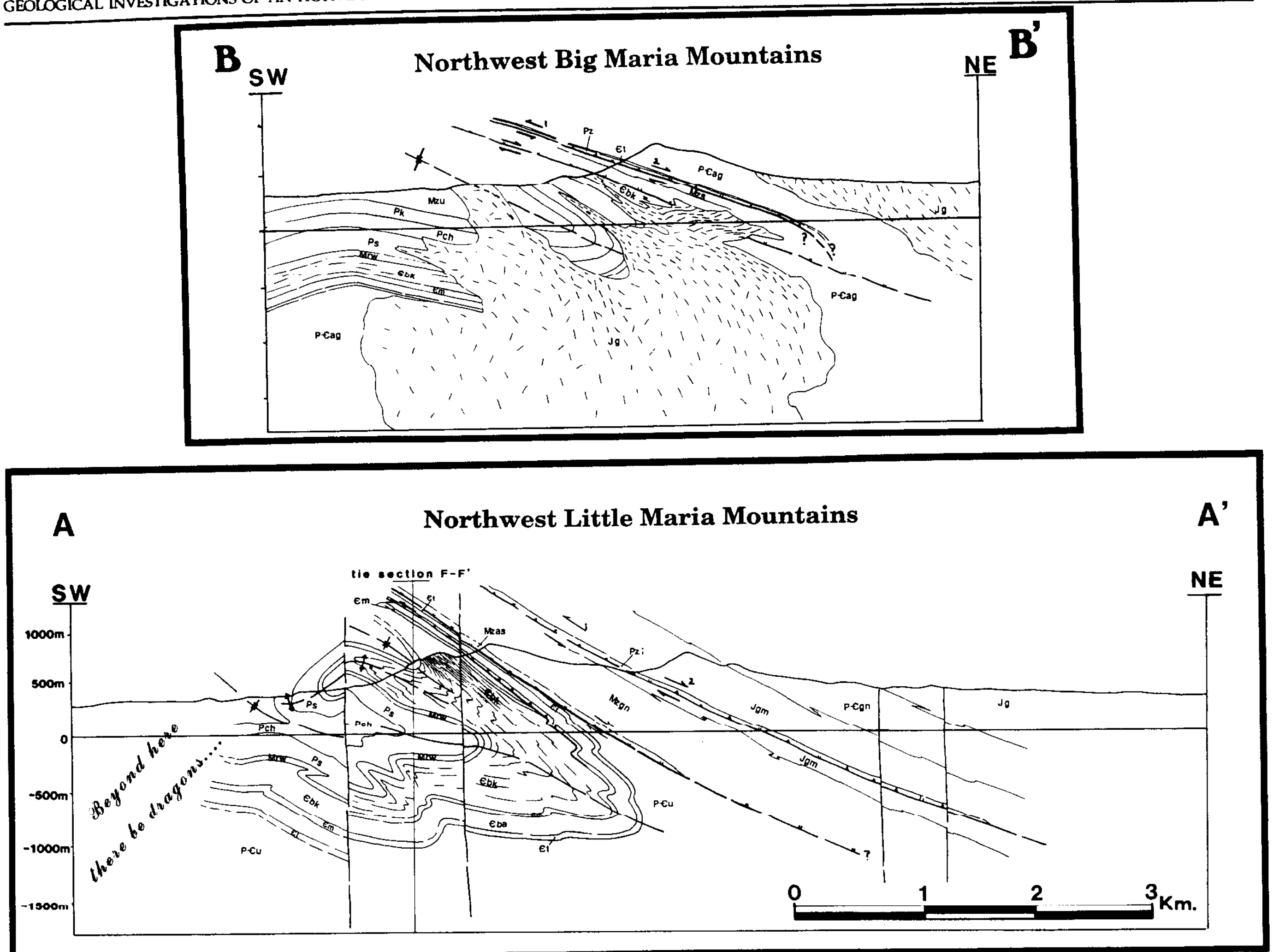

Figure 13. Cross-sections of the northwestern Big Maria Mountains (A-A') and western Little Maria Mountains (B-B'), showing fold geometry. The cross-sections are drawn parallel to D_2 and D_3 tectonic transport (NE-SW) and show the three structural plates. Abbreviations for map units (alphabetic order): Cba-Bright Angel schist (Cambrian), Cbk-Bonanza King(?) marble (Cambrian to Devonian(?)), Cm-Muav marble (Cambrian), Ct-Tapeats quartzite (Cambrian), Jg-granitoid (Jurassic), Jgm-granitoid tectonite (Jurassic(?)), Mrw-Redwall marble (Mississippian), Mzas-actinolite schist (Mesozoic), Mzgn-gneiss (Mesozoic), Mzs-metasedimentary rocks (lower Mesozoic), Mzu-schist and anhydrite (Triassic and Jurassic(?)), pCag-augen gneiss (Precambrian), pCgn-gneiss (Precambrian), pCu-undivided gneiss and granitoid (Precambrian), Pch-Coconino quartzite and Hermit schist (Pennsylvanian(?)-Permian), Pk-Kaibab marble (Permian), Ps-Supai formation (Pennsylvanian-Permian), Pzl-quartzite, schist and marble (lower Paleozoic).

20.8 Fork, KEEP LEFT towards Arlington mine.

21.6 Pass left turn to Arlington Mine.

21.7 TURN RIGHT (north).

22.2 TURN LEFT (west).

23.0 MERGE with road from left, continue straight (west).

23.3 TURN RIGHT, cross major wash system (tricky).

23.6 TURN RIGHT. On north side of braided wash, look for track to north.

27.0 PARK at south end of first high hill. **Stop 3-7. Style of D2 deformation** (Ballard). This stop is the best example of the extreme ductility of D_2 deformation and the complexity of lower plate structure. Figure 13 shows a cross section through this area. The western equivalent of the Little Maria Syncline is exposed with the dark brown Supai Formation occupying the hinge zone. The Mississippian Redwall Formation crops out as a 15-20 m thick, massive white calcite marble and is an excellent marker unit. The middle plate and upper plate here are similar to those in the western Big Maria Mountains (Stop 3-5), but cannot be seen from here. A post-D_2, Late Cretaceous(?) granitoid named the Little Maria Pluton, cuts across D_2 mylonitic fabric and structure at a high angle at the western tip of the range. D_2 mylonite is ubiquitous in this area. The rocks contain excellent L-S and transitional-L fabrics, but no usable kinematic indicators were found in outcrop or thin section. Along major lithologic contacts, D_3 mylonitic fabric overprints D_2 mylonite, and strong C/S fabric, preferred orientation and remnant shape fabric can be observed. The differences in the fabrics reflect changes in the heat flow and availability of water during the D_2 and D_3 phases of deformation.

ACKNOWLEDGEMENTS

Thanks to Steve Reynolds, Nancy Riggs and Jon Spencer for reviewing the manuscript duing the Christmas holidays;

their input significantly improved the manuscript. Paul Fitzgerald kindly made his laserwriter available for printing the final versions of Figures 1-7 and 9-10.

REFERENCES

Ballard, S. N., 1990, The structural geology of the Little Maria Mountains, Riverside County, California [Ph.D. Dissertation]: Santa Barbara, California, University of California, 206 p.

Busby-Spera, C. J., Mattinson, J. M., Riggs, N. R., and Schermer, E. R., 1990, The Triassic-Jurassic magmatic arc in the Mojave-Sonoran Deserts and the Sierra-Klamath region; similarities and differences in paleogeographic evolution, *in* Harwood, D. S., and Miller, M. M., Editors, Paleozoic and early Mesozoic paleogeographic relations; Sierra Nevada, Klamath Mountains, and related terranes, Geological Society of America Special Paper 255, p. 325-337.

Crowl, W. J., 1979, Geology of the central Dome Rock Mountains, Yuma county, Arizona [M. S. thesis]: Tucson, Arizona, University of Arizona, 76 p.

Davis, G., 1985, Geology of the southern Plomosa Mountains [M. S. thesis]: Phoenix, Arizona, Arizona State University, 159 p.

Dickinson, W. R., Fiorillo, A. R., Hall, D. L., Monreal, R., Potochnik, A. R., and Swift, P. N., 1989, Cretaceous strata of southern Arizona, *In* Jenney, J. P., and Reynolds, S. R., editors, Summary of Arizona Geology, Arizona Geological Society Digest, V. 17, p. 447-462.

Flinn, D., 1965, On the symmetry principle and the deformation ellipsoid: Geological Magazine, v. 102, p. 36-45.

Hamilton, W., 1982, Structural evolution of the Big Maria Mountains, northeastern Riverside County, southeastern California, *In* Frost, E. G., and Martin, D. L., editors, Mesozoic-Cenozoic tectonic evolution of the Colorado River region, California, Arizona, and Nevada (Anderson-Hamilton Volume): San Diego, California, Cordilleran Publishers, p. 1-28.

Hamilton, W., 1984, Generalized geologic map of the Big Maria Mountains region, northeastern Riverside County, southeastern California: U. S. Geological Survey Open-File Report 84-407, scale 1:48000.

Hamilton, W., 1987, Mesozoic geology and tectonics of the Big Maria Mountains region, southeastern California, *in* Dickinson, W. R., and Klute, M. A., editors, Mesozoic geology of southern Arizona and adjacent areas, Arizona Geological Society Digest, V. 18, p. 33-47.

Harding, L. E., 1982, Tectonic significance of the McCoy Mountains formation, southeastern California and southwestern Arizona [Ph.D. Dissertation]: Tucson, Arizona, University of Arizona, 197 p.

Harding, L. E., and Coney, P. J., 1985, The geology of the McCoy Mountains formation, southeastern California and southwestern Arizona: Geological Society of America Bulletin, v. 96, p. 755-769.

Harrison, T. M., Duncan, I., and McDougall, I., 1985, Diffusion of 40Ar in biotite: Temperature, pressure and compositional effects: Geochimica et Cosmochimica Acta, v. 49, p. 2461-2468.

Hoisch, T. D., 1985, Metamorphism in the Big Maria Mountains, southeastern California [Ph.D. dissertation]: Los Angles, California, USC, 264 p.

Hoisch, T. D., 1987a, Heat transport by fluids during Late Cretaceous regional metamorphism in the Big Maria Mountains, southeastern California: Geological Society of America Bulletin, v. 98, p. 549-553.

Hoisch, T. D., 1987b, Conditions of Late Cretaceous regional metamorphism in the Little Maria Mountains, southeastern California, Geological Society of America, abstracts with programs, V. 19, no. 6, p. 389.

Hoisch , T.D., 1991, The Thermal Effects of Pervasive and Channelized Fluid Flow in the Deep Crust: Journal of Geology, v. 99, p. 69-80.

Hoisch, T. D., and Hamilton, W., 1990, A granite origin by fluid-induced anatexis, *in* Miller, C. F., Editor: Transactions of the American Geophysical Union, v. 71, p. 694.

Hoisch, T. D., Miller, C. F., Heizler, M. T., Harrison, T. M., and Stoddard, E. F., 1988, Late Cretaceous regional metamorphism in southeastern California, *in* W. G. Ernst, editor, Metamorphism and crustal evolution of the western United States (Rubey Vol. 7): Englewood Cliffs, New Jersey, Prentice-Hall Inc., p. 538-571.

Holdaway, M. J., 1971, Stability of andalusite and the aluminum silicate phase diagram: American Journal of Science, v. 271, p. 97-131.

Knapp, J. H., 1989, Structural development, thermal evolution, and tectonic significance of a Cordilleran basement thrust terrane, Maria fold and thrust belt, west-central Arizona [Ph.D. Dissertation]: Cambridge, MA, Massachusetts Institute of Technology, 261 p.

Knapp, J. H., and Heizler, M. T., 1990, Thermal history of crystalline nappes of the Maria fold and thrust belt, west central Arizona: Journal of Geophysical Research, v. 95, p. 20049-20073.

Lawton, T. F., McMillan, N. J., and Cameron, K. L., 1993, Late Jurassic extension in the Bisbee Basin: Marine and volcanic strata of the Chiricahua Mountains, Arizona, Geological Society of America, abstracts with programs, V. 25, no. 5, p. 68.

Lerch, M. F., 1990, Geologic mapping and isotopic studies in the Quartzsite region, west-central Arizona: Implications for Proterozoic and Mesozoic tectonics [M. S. thesis]: Tucson, Arizona, University of Arizona, 104 p.

Lerch, M. F., Patchett, P. J., and Reynolds, S. J., 1991, Sr and Nd isotopic studies of Proterozoic rocks in west-central Arizona: Implications for Proterozoic tectonics, *in* Karlstrom, K. E., ed., Proterozoic Geology and Ore Deposits of Arizona, Arizona Geological Society Digest 19: Tucson, Arizona, p. 51-56.

Marin, B., 1993, Kinematic evolution of a ductile shear zone system, Granite Wash Mountains, West Central Arizona [M.A. Thesis]: Austin, Texas, Univ. of Texas, 131 p.

Martin, D. L., Krummenacher, D., and Frost, E. G., 1982, K-Ar geochronologic record of Mesozoic and Tertiary tectonics of the Big Maria-Little Maria-Riverside Mountains terrane, *in* Frost, E. G., and Martin, D. L., editors, Mesozoic-Cenozoic tectonic evolution of the Colorado River region, California, Arizona, and Nevada (Anderson-Hamilton Volume): San Diego, California, Cordilleran Publishers, p. 518-549.

Miller, F. K., 1970, Geologic map of the Quartzsite Quadrangle, Yuma County, Arizona: U. S. Geological Survey Geological Quadrangle Map GQ-841, scale 1:62500.

Miller, F. K., and McKee, E. H., 1971, Thrust and strike-slip faulting in the Plomosa Mountains southwestern Arizona: Geological Society of America Bulletin, v. 82, p. 717-722.

Miller, W. J., 1944, Geology of the Palm Springs-Blythe strip, Riverside County, California, California Journal of Mines and Geology 40, p. 11-72.

Pelka, G. J., 1973, Geology of the McCoy and Palen Mountains, southeastern California [Ph.D. Dissertation]: Santa Barbara, California, University of California, 160 p.

Reynolds, S. J., Spencer, J. E., Asmerom, Y., DeWitt, E., and Laubach, S. E., 1989, Early Mesozoic uplift in west-central Arizona and southeastern California: Geology, v. 17, p. 207-211.

Reynolds, S. J., Spencer, J. E., Richard, S. M., and Laubach, S. E., 1986, Mesozoic structures in west-central Arizona, *in* Beatty, B., and Wilkinson, P. A. K., editors, Frontiers in geology and ore deposits of Arizona and the Southwest, Arizona Geological Society Digest 16, p. 35-51.

Rice, J. M., 1977, Progressive metamorphism of impure dolomitic limestone in the Marysville aureole, Montana: American Journal of Science, v. 277, p. 1-24.

Richard, S. M., 1992a, Bedrock geologic map of the Imperial Reservoir Quadrangle, Yuma County, Arizona and Imperial County, California: Arizona Geological Survey Open-file Report 92-11, Tucson, scale 1:24000.

Richard, S. M., 1992b, Detailed Geologic map of the upper Apache Wash Area, central southern Plomosa Mountains, West-central Arizona: Arizona Geological Survey Open-file Report 92-2, 1 sheet, 11 pages, scale 1:12000.

Richard, S. M., 1993, Palinspastic reconstruction of southeastern California and southwestern Arizona for the Middle Miocene: Tectonics, v. 12, p. 830-854.

Richard, S. M., Reynolds, S. J., and Spencer, J. E., 1987, Mesozoic stratigraphy of the Little Harquahala and Harquahala Mountains, west-central Arizona, *in* Dickinson, W. R., and Klute, M. A., editors, Mesozoic geology of southern Arizona and adjacent areas, Arizona Geological Society Digest, V. 18, p. 101-120.

Richard, S. M., Spencer, J. E., Tosdal, R. M., and Stone, P., 1993, Preliminary geologic map of the southern Plomosa Mountains, La Paz County, Arizona: Open-file Report 93-9. Tucson, Arizona, Arizona Geological Survey, 1 sheet, 27 pages , scale 1:24000.

Riggs, N. R., Mattinson, J. M., and Busby, C. J., 1993, Correlation of Jurassic eolian strata between the magmatic arc and the Colorado Plateau: New U-Pb geochronologic data from southern Arizona: Geological Society of America Bulletin, v. 105, p. 1231-1246.

Sherrod, D. R., Koch, R. D., and Grubensky, M. J., 1990, Geologic Map of the Vicksburg quadrangle, La Paz County, Arizona: U. S. Geological Survey Geological Quadrangle Map GQ-1684, scale 1:62500.

Sherrod, D. R., and Tosdal, R. M., 1991, Geologic Setting and Tertiary Structural Evolution of Southwestern Arizona and Southeastern California: Journal of Geophysical Research, v. 96, p. 12407-12423.

Spencer, J. E., and Reynolds, S. J., 1989, Middle Tertiary tectonics of Arizona and adjacent areas, *in* Jenney, J. P., and Reynolds, S. J., Editors, Geologic Evolution of Arizona, Arizona Geological Society Digest 17: Tucson, p. 539-574.

Spencer, J. E., and Reynolds, S. J., 1991, Tectonics of mid-Tertiary extension along a transect through west central Arizona: Tectonics, v. 10, p. 1204-1221.

Stone, P., 1990, Preliminary Geologic map of the Blythe 30′ by 60′ quadrangle, California and Arizona: U. S. Geological Survey Open-File Report 90-497, scale 1:100000.

Stone, P., Page, V. M., Hamilton, W., and Howard, K. A., 1987, Cretaceous age of the McCoy Mountains Formation, southeastern California and southeastern Arizona: Geology, v. 15, p. 561-564.

Tosdal, R. M., 1986, Mesozoic ductile deformations in the southern Dome Rock Mountains, northern Trigo Mountains, Trigo Peak and Livingston Hills, southwestern Arizona, and Mule Mountains, southeastern California, *in* Beatty, B., and Wilkinson, P. A. K., editors, Frontiers in Geology and Ore Deposits of Arizona and the Southwest, Arizona Geological Society Digest, V. 16, p. 62-71.

Tosdal, R. M., 1990a, Constraints on tectonics of the Mule Mountains thrust system, southeast California and southwest Arizona: Journal of Geophysical Research, v. 95, p. 20,025-20,048.

Tosdal, R. M., 1990b, Jurassic low-angle ductile shear zones, SE California and SW Arizona: Thrust faults, extensional faults or rotated high-angle faults?, Geological Society of America, abstracts with programs, V. 22, no. 3, p. 89.

Tosdal, R. M., and Stone, P., 1994, Stratigraphic relations and U-Pb geochronology of the Upper Cretaceous McCoy Mountains Formation, southwestern Arizona: Geological Society of America Bulletin. in press.

Tosdal, R. M., Haxel, G. B., and Wright, J. E., 1989, Jurassic geology of the Sonoran Desert region, southern Arizona, southeast California, and northernmost Sonora: Construction of a continental-margin magmatic arc, *in* J.P. Jenny, and S.J. Reynolds, editors, Summary of Arizona Geology, Arizona Geological Society Digest, V. 17, p. 397-434.